Available online at www.sciencedirect.com
ScienceDirect
Applied Geochemistry 22 (2007) 692–714
Applied Geochemistry
www.elsevier.com/locate/apgeochem

^{129}I and ^{36}Cl in dilute hydrocarbon waters: Marine-cosmogenic, *in situ*, and anthropogenic sources

Glen T. Snyder [a,*], June T. Fabryka-Martin [b]

[a] *Earth Science Department, Rice University, Houston, TX 77251-1892, United States*
[b] *Hydrology, Geochemistry and Geology Group, Los Alamos National Laboratory, Los Alamos, NM 87545, United States*

Available online 22 December 2006

Abstract

The long-lived halogen radioisotopes ^{129}I and ^{36}Cl provide valuable information regarding the source of fluids in hydrocarbon systems and in localized areas where infiltration of younger meteoric water has occurred. Despite the utility of these two isotopes in providing time-signatures for fluid end-members, considerable uncertainty remains regarding the interpretation of ''intermediate-age'' waters in hydrologic systems. These waters are likely the result of the combination of two or more halogen sources at some time in the past, each with its own characteristic concentration and isotopic composition. In order to unravel the evolution of these ''intermediate-age'' waters, the effect that infiltration of meteoric water has on the isotopic composition of older formation waters is modeled. Also evaluated is the effect that the timing of dilution has on ^{129}I and ^{36}Cl signatures observed in the present, specifically, the hypothesis that halogen isotopic signatures imparted by the mixing of brine and meteoric waters early in the development of a sedimentary basin are quantitatively different from those imparted by the mixing of old brines with recent meteoric waters.

The modeled results are compared to previously published isotopic data from production wells in the Fruitland Formation coalbed methane system. Portions of the basin preserve enough of the original brine source to retain $^{129}I/I$ ratios roughly recording the age of deposition of organic matter (73–76 Ma) even where some degree of dilution by meteoric water has occurred. However, the ^{129}I signatures of waters that presently contain less than 10% of the original formation water component indicate that mixing has occurred within the past 10 Ma, consistent with recently published ^{4}He data. Both ^{36}Cl concentrations and $^{36}Cl/Cl$ ratios show that waters containing more than 10% formation water are all in secular equilibrium with the host formation coals. In contrast, waters with less than 1% of the original formation water's Cl^- content all have $^{36}Cl/Cl$ ratios which are greater than secular equilibrium values, indicating the migration of meteoric water into the coal formation more recently than 2 Ma. Although ^{36}Cl signatures in the Fruitland Formation are not significantly affected by anthropogenic input, $^{129}I/I$ ratios in a subset of samples that retain less than 1% of the initial formation water component suggest input of anthropogenic ^{129}I during the past 50 a.

1. Introduction

The element iodine is generally biophilic in oxic aqueous environments such as oceans and lakes, and yet migrates relatively conservatively, in the form of reduced I^-, in anoxic waters (Elderfield

* Corresponding author.
E-mail address: gsnyder@rice.edu (G.T. Snyder).

0883-2927/$ - see front matter © 2006 Elsevier Ltd. All rights reserved.
doi:10.1016/j.apgeochem.2006.12.011

and Truesdale, 1980; Kennedy and Elderfield, 1987; Anschutz et al., 2000). These two characteristics make I a unique tracer in hydrocarbon systems, because the oxidation of organic matter to produce hydrocarbons is generally associated with the nearly-simultaneous release of I^- into marine sediment pore fluids and hydrocarbon-rich groundwater (e.g. Martin et al., 1993; Egeberg and Dickens, 1999). Isotopic studies of I also show great potential in tracing the source and migration of these waters, because I has only two naturally occurring isotopes: long-lived ^{129}I ($t_{1/2} = 15.6$ Ma) and stable ^{127}I. Over the past two decades, progress has been made in bounding the age of the organic source in hydrocarbon brines, based on the assumption that the initial marine-cosmogenic ratio of $^{129}I/I$ has remained fairly constant over time ($1500 \times 10^{-15} \pm 10\%$) and calculating the time required for it to decay to the present observed ratio (Moran et al., 1995; Fehn et al., in press). This approach has been applied to a variety of geologic settings including regions which host gas hydrates (Fehn et al., 2000, 2003; Tomaru et al., 2007), areas of commercial production of coalbed methane (Snyder et al., 2003; Riese et al., 2005), fluid inclusions in salt domes (Fabryka-Martin et al., 1985) and regions where groundwater chemistry is influenced by volcanic-geothermal circulation (Fehn et al., 1992; Snyder et al., 2003; Hurwitz et al., 2005). When combined with other water and gas characteristics, ^{129}I determinations provide valuable insight into the source and migration of fluids (e.g. Fehn et al., 1992; Moran et al., 1995). In other cases, where waters of relatively low ^{127}I concentrations are in prolonged contact with rocks containing even background concentrations of U, the *in situ* production of ^{129}I is sufficient to influence $^{129}I/I$ ratios significantly, providing insight into the residence time of water in the formation (Andrews et al., 1989; Fabryka-Martin et al., 1989; Bottomley et al., 2002; Fehn and Snyder, 2005). Finally, in hydrologic systems fed by recent recharge, the increase of ^{129}I due to anthropogenic nuclear activities is reflected by high $^{129}I/I$ ratios in these young waters. Although other anthropogenic tracers in the atmosphere such as ^3H and ^{36}Cl produced through the surface testing of nuclear devices have largely returned to pre-anthropogenic levels (Cornett et al., 1997; Delmas et al., 2004), the influx of recent water with its enhanced ^{129}I content is readily discernible through accelerator mass spectrometry (AMS) analyses of seawater (e.g. Edmonds et al., 2001; Aldahan et al., 2007 Schnabel et al., 2007), lake and river water (e.g. Fehn and Snyder, 2000; Buraglio et al., 2001; Moran et al., 2002; Atarashi-Andoh et al., 2007) and shallow groundwater (Schwehr et al., 2005).

Because Cl^- behaves conservatively in low-temperature groundwater systems and is generally unaffected by changes in the redox state of natural aqueous systems, the ratios of Cl^- to other aqueous species such as Br^- have been the subject of numerous studies pointing to the source and mixing of groundwater end-members (e.g. Farber et al., 2007). Investigations of a second long-lived halogen isotope, ^{36}Cl ($t_{1/2} = 301$ ka) can further elucidate the migration of fluids in groundwater systems. As with ^{129}I, studies over the past 20 a have included basin waters (Bentley et al., 1986; Fabryka-Martin et al., 1991; Nolte et al., 1991; Lehmann et al., 2003), coalbed methane brines (Snyder et al., 2003), fracture fluids (Andrews et al., 1986, 1989; Lippmann et al., 2003; Fehn and Snyder, 2005), geothermal systems (Hedenquist et al., 1990; Fehn et al., 1992; Rao et al., 1996) and also water from wells and springs (Davis et al., 2000, 2001; Rao et al., 2005). Unlike $^{129}I/I$ ratios, $^{36}Cl/Cl$ ratios in seawater are below the detection limit of AMS ($\sim 2 \times 10^{-15}$, Sharma et al., 2000). Due to the shorter half-life of ^{36}Cl, old groundwater which still contains a significant fraction of its initial marine-cosmogenic ^{129}I signature may only have ^{36}Cl derived from *in situ* nucleogenic production. Although the production mechanisms of *in situ* ^{129}I and ^{36}Cl differ in fundamental ways, their relative production rates have been discussed in the context of other nucleogenic, radiogenic and fissiogenic isotopes such as ^3H, ^4He, and ^{81}Kr (Andrews et al., 1991; Lehmann et al., 2003).

Although ^{129}I and ^{36}Cl have been useful for constraining the age and source of meteoric and formation water end-members, both uncertainty and debate remain associated with interpretation of samples which show intermediate $^{129}I/I$ and $^{36}Cl/Cl$ values. When distributed across broad regions, these intermediate values could result from multiple processes including: admixing of recent and formation waters, minor additions of anthropogenic waters to formation waters, dissolution of halite or leaching of old organic material from rocks and sediments, or leaching of *in situ*-produced ^{129}I and ^{36}Cl from rocks and sediments. The distinctions among these different processes are neither clearcut nor trivial, and interpretations of the signals are also subject to our understanding of the extent to which

sampled groundwater reside in a compartmentalized system of different ^{129}I and ^{36}Cl "ages", or derive from a single interconnected regional flow system.

Samples from the Fruitland Formation coalbed methane system of the San Juan Basin exemplify the complexities involved in groundwater dating. In the central, overpressured portion of the basin, $^{36}Cl/Cl$ values in the older brines are at secular equilibrium with the host formation, while $^{129}I/I$ ratios (Snyder et al., 2003) coincide both with the age of the coals (Fassett, 2000), as well as with fluid residence times determined by the accumulation of ^{4}He (Sorek, 2003). In contrast, towards the western edge of the basin, ages based solely on the radioactive decay of the marine-cosmogenic ^{129}I component are younger than the host coals, but still significantly older than those based on the decay of ^{36}Cl (Snyder et al., 2003; Riese et al., 2005) and the accumulation of ^{4}He (Zhou and Ballentine, 2006). This apparent disparity among ages derived from different dating methods is by no means unique to the Fruitland Formation (e.g. Fabryka-Martin et al., 1991; Lehmann et al., 2003) and has even been observed in the bottom waters of modern brine lakes (Poreda et al., 2004; Lyons et al., 2005). The classic concept of groundwater "age" must therefore be modified for time-sensitive tracers to account not only for the decay and *in situ* production of ^{36}Cl, ^{129}I and ^{4}He, but also for variable degrees of mixing of end-members of different isotopic composition (Bethke et al., 2000).

This paper focuses on reconstructing the evolutionary pathway that produced the ^{129}I and ^{36}Cl signatures observed in the dilute hydrocarbon waters of the Fruitland Formation, across southern Colorado and northern New Mexico. Although the principles presented are applicable to a number of different settings, the Fruitland Formation provides the largest published database of ^{129}I and ^{36}Cl values for a single hydrocarbon basin. Among types of hydrocarbon accumulations, coalbed methane systems are also comparatively simple, because the hydrocarbon source and its trap are one and the same formation (Levine, 1993). The data presented in this paper were collected as part of a basin-wide hydrologic modeling project (3M Project, 2000) and are published in Riese et al. (2005) and Snyder et al. (2003). Although these publications provide a qualitative discussion of the mixing of formation waters and meteoric waters, this paper uses ^{129}I and ^{36}Cl data to model the evolution of these mixed fluids over time. This paper is the first to investigate the hypothesis that halogen isotopic signatures imparted by the mixing of brine and meteoric waters early in the development of the basin are quantitatively different from those imparted by the mixing of old brines with recent meteoric waters.

2. Geological and hydrologic setting

The Upper Cretaceous Fruitland Formation of the San Juan Basin is presently the second largest gas producing basin in the United States, with total reserves estimated at $1.4 \times 10^9\ m^3$ (Choate et al., 1984; Kuuskraa and Boyer, 1993; Fassett, 2000). As such, the basin is also one of the most extensively studied in the world, with a wealth of information available from chemical and isotopic investigations (Scott et al., 1994; Snyder et al., 2003; Riese et al., 2005; Zhou et al., 2005; Zhou and Ballentine, 2006), geophysical logging (Clarkson et al., 1988; McCord et al., 1992) and well production histories extending over 25 a. The Fruitland coals themselves reach thicknesses of 30 m, and consist of a series of discontinuous beds. These coals were initially deposited as peats behind the shoreline of the Western Interior Seaway between 76 Ma and 73 Ma. During this time, shoreline migrations coupled with fluctuations in sedimentation rates resulted in stepwise, shingled interbedding between the Fruitland coals and marginal marine sandstones of the Pictured Cliffs Formation (Scott et al., 1994; 3M Project, 2000; Fassett, 2000). Uplift of the northern margin of the basin was initiated during the Oligocene at 35–25 Ma (Clarkson et al., 1988) and produced buckling of the basement rock and development of the present basin hingeline whose axis crops out roughly 10 km north of the Colorado–New Mexico state line, and extends to the SE in New Mexico (Fig. 1) (Choate et al., 1984; Fassett, 2000). High vitrinite-reflectance coals, hosting groundwaters rich in dissolved halides, are located to the north of both the state line and the structural hingeline, and represent the lowermost portion of the basin prior to uplift (Fassett, 2000; Snyder et al., 2003).

In the late 1970s, it was discovered that coalbeds in the region host large amounts of natural gas derived from both biogenic and thermogenic processes within the coals (Scott et al., 1994) and that the gas is retained in the coals by fluid overpressures. Since then, commercial production of this unconventional gas resource has generally involved hydrofracturing the coals to increase permeability

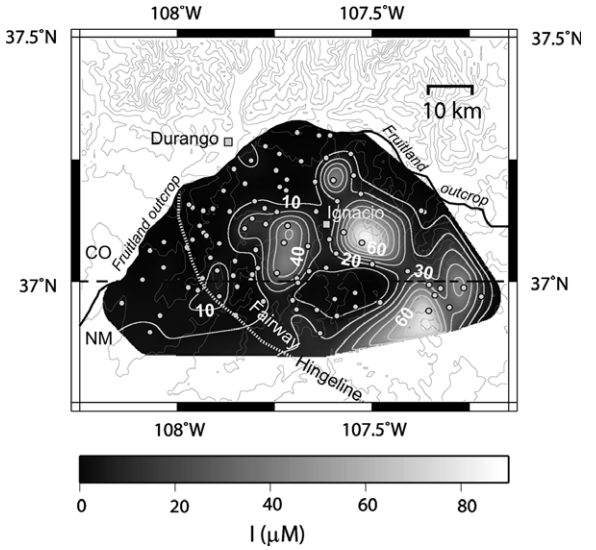

Fig. 1. Spatial distribution of dissolved I concentrations in the Fruitland Formation coals, northern San Juan Basin (after Snyder et al., 2003). Circles show sampled production wells. Formation outcrop indicated by the solid black line, the dashed black line along the 37th parallel indicates the Colorado–New Mexico state line. White dotted diagonal trending from NW to SW shows the approximate position of the present structural hinge line. The high production "Fairway" is located just to the north of the structural hinge line. Iodine concentrations reach a maximum (109 μM) near the village of Ignacio.

(Palmer et al., 1993), and then pumping off the water to induce gas desorption (Choate et al., 1984; Schraufnagel, 1993). Areas of major interest for gas production include the San Ignacio region, located in the northern portion of the basin, which hosts the high vitrinite-reflectance coals, and the coalbed-methane high-productivity "Fairway", a 20-km wide zone of thick coals and groundwater overpressure which runs parallel to and north of the structural hingeline (Fig. 1). In the mid-1990s, the total number of production wells in both areas exceeded 3000 and the cumulative amount of produced water from the coals exceeded $4 \times 10^7\ m^3$. This high extraction rate prompted the residents of the area to express a number of environmental concerns, including the possibility that the drawdown of the water table would exacerbate problems of contamination of well water, coal fires and tree-kills (Bureau of Land Management, 1999; Gorody, 2001).

In order to assess environmental impact, the Colorado Oil and Gas Conservation Commission, in conjunction with the Bureau of Land Management, initiated the 3M Project with the objectives of modeling the hydrology of the Fruitland Formation in both present and pre-production conditions, and then projecting the response to different scenarios through the course of commercial production (3M Project, 2000). Three possible hydrologic scenarios are contemplated in the model. In the first, the coalbeds are considered to comprise an essentially open artesian system, where overpressures are produced in the center of the basin by the present topographic relief, recharge is focused in the north of the basin, and discharge is to the south. In the second, the structural hingeline is considered to be a hydrologic barrier, impeding basin-wide throughflow in an otherwise open system. In the third scenario, the system is considered to be highly compartmentalized, with fluid overpressures preserved in some of the compartments from a time prior to basin uplift. Proponents of the first scenario cite a number of lines of evidence including: presence of secondary microbially derived gases in portions of the basin (Scott et al., 1994), thermal evidence for lateral advection (McCord et al., 1992), low Cl^- concentrations in portions of the northern basin (Scott et al., 1994), and high permeability based on production tests of hydrofractured wells. Proponents of the second scenario cite evidence of an abrupt transition from an overpressured system to the north to an underpressured system to the south of the hingeline, as well as distinctly different water and gas compositions on each side (Rice, 1993; Scott et al., 1994; Zhou et al., 2005). Finally, proponents of the compartmentalized scenario cite abrupt differences in production histories of adjacent wells, numerous discontinuities in the coals themselves, water chemistries that parallel syndepositional structures, and evidence that authigenic mineralization makes the coals less permeable than would otherwise be predicted (Riese et al., 2005).

In the course of modeling the hydrology of the San Juan Basin (3M Project, 2000) and in studies which have followed, a number of discrepancies have arisen regarding the appropriate application of isotopic age-dating. There is general agreement that production well waters from portions of the basin yield quite old isotopic signatures. The portion of the Fruitland Formation that appears to have undergone the least amount of exchange with meteoric water appears to be the San Ignacio region to the north of the structural hingeline. There, Cl^- and I^- concentrations are high (Fig. 1), as are ^4He ages (Sorek, 2003) as well as ^{129}I ages (Snyder et al., 2003; Riese et al., 2005), which both extend

into the tens of millions of years (Fig. 2). Values of $^{36}Cl/Cl$ in the same region indicate secular equilibrium with the *in situ* neutron flux, and provide corroborating evidence that the residence time is longer than a million years. In contrast, overpressured regions near the Fairway yield ^{4}He ages determined to be 100 ka at a distance of 5 km from the western outcrop and that increase to nearly 500 ka at greater distances from the western outcrop (Zhou and Ballentine, 2006). Across the same area included in the ^{4}He study, ^{129}I ages, based solely on the decay of the marine-cosmogenic signature, range from anthropogenic values (i.e. less than 50 a) to as old as 30 Ma (Snyder et al., 2003).

The arguments, "reinterpretations", and rebuttals that have ensued as a result of these age discrepancies in the San Juan Basin bear striking resemblance to a flurry of papers published a decade earlier in *Applied Geochemistry* and *Journal of Hydrology*. These earlier discussions were instigated primarily by the publication of two studies (Mazor, 1992; Mazor and Nativ, 1992) which "reinterpreted" previously published ^{36}Cl data (Bentley et al., 1986; Phillips et al., 1986) to indicate the presence of essentially static or "dead" volumes of water throughout the Great Artesian Basin of Australia and the Milk River Aquifer of Alberta, Canada. These papers elicited a variety of discussion papers

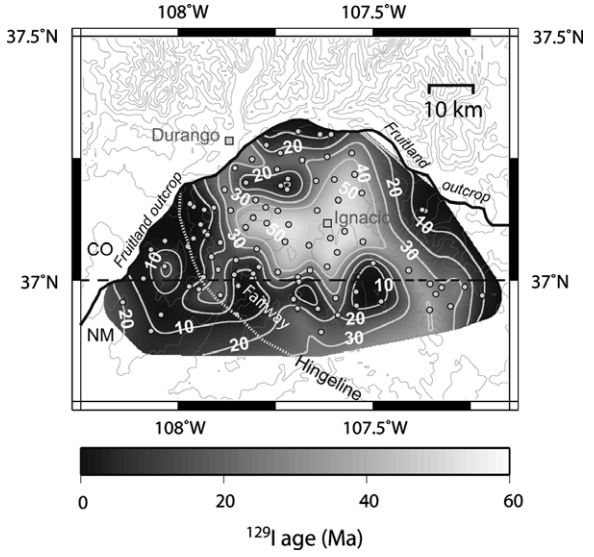

Fig. 2. Distribution of apparent ^{129}I ages, based on Eq. (1) (After Riese et al., 2005). The oldest apparent ages (samples with low $^{129}I/I$ ratios) are focused in the areas of high I concentrations. Apparent ages in the intermediate range radiate from the areas of old ^{129}I ages.

(Fontes and Andrews, 1993; Kellett et al., 1993; Phillips, 1993; Torgersen, 1994) pointing to evidence that ^{36}Cl varies systematically with distance from the edge of the basins and that these changes are consistent with existing conceptual models of basin flow as well as a variety of other chemical and isotopic data. These papers were accompanied by a number of replies (Mazor, 1993a,b; Mazor and Nativ, 1994) which focused on depositional and structural aspects common to basins, as well as on assumptions of hydraulic entrapment that have long been espoused by the petroleum industry.

Although the arguments set forth in the early 1990s did not achieve any consensus within the hydrological community, they did underscore the fact that simple piston-flow modeling cannot adequately explain discrepancies in the isotope ages of groundwater. Subsequent flow and solute transport models have taken into account other mechanisms that affect isotopic distributions, such as diffusion, advection, and hydrodynamic dispersion (Bethke et al., 2000; Park et al., 2002). The approach taken in this paper is to consider exchange between dilute waters of meteoric origin with halide-rich formation waters, both in the past and the present. By considering the hypothesis that halogen isotopic signatures will evolve differently if meteoric waters were flushed through the system millions of years ago as opposed to recently, this study should serve to corroborate or refute earlier concepts. Old mixing times would strongly support hydrological isolation, either during diagenesis or during basin uplift, and would suggest effective compartmentalization within the coals. In contrast, young mixing times would indicate active exchange between recent recharge waters and old brines.

3. ^{129}I sources in coalbed systems

3.1. The marine-cosmogenic ^{129}I signature

In order to assess the residence time of I present in hydrocarbon systems, an initial input value of $^{129}I/I$ must be assumed. Early estimates of the steady-state $^{129}I/I$ ratio in the hydrosphere, based on a mass balance of ^{129}I fluxes from cosmic-ray production, volcanic emissions, and other sources, range from 3×10^{-13} to 3×10^{-12} (Fabryka-Martin et al., 1985). Subsequently, $^{129}I/I$ ratios determined for shallow marine sediments (Moran et al., 1998) and those determined for seaweed that was archived over a century ago (Fehn et al., in press), coincide at

$1500 \times 10^{-15} \pm 10\%$. Pre-anthropogenic ratios have also been preserved in cores taken from living corals (Biddulph et al., 2006). Because the residence time of I in the oceans is quite long (~300 ka, Broecker and Peng, 1982), the marine-cosmogenic ^{129}I/I signature is assumed to be well mixed with regards to any latitudinal or temporal variations that might have occurred in cosmogenic production and deposition throughout the time period of interest for this study. Iodine is transported from the oceans to the atmosphere via seaspray and volatilization of organohalides by bacteria (Amachi et al., 2001) or by phytoplankton (Carpenter et al., 1999; Greenberg et al., 2005). On the land surface, I in surface waters and terrestrial organic matter is derived from wet and dry deposition of marine seaspray and from photolysis of marine-derived organics, with atmospheric residence times ranging from days to a few years. Because of the dominance of the marine source term even for locations remote from any ocean, pre-anthropogenic groundwaters are also assumed to have the same initial marine-cosmogenic ratio as seawater.

Several portions of the Fruitland Formation to the north of the Fairway and of the New Mexico–Colorado state line host moderately elevated Cl^- concentrations (73 mM) as well as the highest I concentrations measured in the local groundwaters (109 μM). Although the general brackish nature of these groundwaters probably results from dilution of formation waters that were initially similar to seawater, the dissolved I contents are enriched by over two orders of magnitude relative to seawater, which is assumed to be due to the release of I from the peat deposits during the coalification process (Snyder et al., 2003).

The same area hosts the lowest ^{129}I/I ratios ($<150 \times 10^{-15}$). Ignoring any effects of mixing and *in situ* production of ^{129}I, the observed I isotopic ratio is a function of the burial time, as expressed by the simple decay equation:

$$R_{obs} = R_i e^{-\lambda_{129} t}, \quad (1)$$

where R_{obs} is the present observed ^{129}I/I ratio, R_i is the initial value (1500×10^{-15}), the decay constant λ_{129} is 4.41×10^{-8} a^{-1}, and t is the time elapsed since burial of the coal-forming peats. Using this approach, ^{129}I decay ages for these oldest samples in the Fruitland Formation exceed 50 Ma. Both the Fairway and most of the study area south of the state line have apparently younger ^{129}I-based ages (Fig. 2). As with other isotopic systems (Bethke et al., 2000), the mixing of formation waters with younger groundwaters in fairly open hydrologic systems may impart a net ^{129}I/I signature that can be easily misinterpreted as characteristic of intermediate-age groundwaters. With the exception of a few cases south of the state line, the younger "ages" and higher ^{129}I/I ratios are coupled with both lower Cl^- and I^- concentrations. The exceptions include areas with low I^- concentrations accompanied by high Cl^- concentrations and high ^{129}I/I ratios. These anomalies are found in the southern portion of the study area, situated between the state line and the structural hingeline, and may be related to thinning of the coalbeds (Riese et al., 2005). As will be discussed, if the initial I contents were low in these cases, then any contribution of ^{129}I from other sources will have a proportionately larger effect on the ^{129}I/I ratio and hence would decrease the apparent "age".

3.2. *In situ* ^{129}I production, escape efficiency, and excess

In situ production of ^{129}I within rock formations is due to spontaneous fission of ^{238}U. The presence of *in situ* produced ^{129}I in old groundwaters has been well documented in the fracture fluids of granites and other U-rich host rocks (Andrews et al., 1989; Fabryka-Martin et al., 1989; Bottomley et al., 2002; Fehn and Snyder, 2005), in which cases fissiogenic ^{129}I manifests itself by increasing the ^{129}I/I ratio well above the level expected if only the marine-cosmogenic component were present. In I-rich systems younger than 30 Ma, the marine-cosmogenic component generally dominates over the fissiogenic component (e.g. Moran et al., 1995; Muramatsu et al., 2001; Fehn et al., 2000; Snyder and Fehn, 2002). The influence of *in situ* production on ^{129}I/I ratios in waters with only low I levels may be significant, however, because the fissiogenic production of ^{129}I is independent of the amount of stable I in solution. The amount of fissiogenic ^{129}I accumulated in groundwater as a function of time – referred to as "excess ^{129}I" in this paper – may be expressed as (Fabryka-Martin et al., 1989):

$$N_{129} = N_{238} \lambda_{sf} Y_{129} \varepsilon \rho \{(1-\phi)/\phi\}(1 - e^{-\lambda_{129} t})/\lambda_{129}, \quad (2)$$

where $N_{129} = {}^{129}$I atoms/L-fluid, $N_{238} = {}^{238}$U-atoms/kg-rock, λ_{sf} = spontaneous fission decay constant for ^{238}U (8.5×10^{-17} a^{-1}, Decarvalho et al., 1982),

Y_{129} = spontaneous fission yield of ^{238}U at mass 129 (3×10^{-4}; Hebeda et al., 1987), ε = escape efficiency of ^{129}I from the mineral lattice into the fluid, ρ = rock density, ϕ = effective porosity, λ_{129} = decay constant for ^{129}I (4.41×10^{-8} a^{-1}), t = residence time of fluids in contact with the rocks.

For the purposes of this investigation, coal density is assumed to be 1.79 g/cm^3 (Zhou and Ballentine, 2006) and effective porosity to be 0.01 (Young et al., 1991; 3M Project, 2000; Sorek, 2003). In such cases, where the effective porosity is $\ll 1$, the term $\{(1-\phi)/\phi\}$ in Eq. (2) reduces to $(1/\phi)$. A mean U concentration in the coals of 2.8 ppm (11.8 μmol/kg) is assumed (Zhou and Ballentine, 2006).

The escape efficiency (ε) is an expression of the fractional release of a given radioisotope produced within a mineral or maceral and transferred into the fluid phase. Factors influencing ε-values include diagenetic alteration, metamorphism, degree of fracturing, and other physical alterations of the mineral surfaces that affect grain size. Diffusivity, as well as the retentivity of different isotopes within the mineral lattices, can also strongly influence their escape efficiencies (Torgersen, 1980; Torgersen et al., 2004). Thus, even though the escape efficiency of radiogenic ^4He in the Fruitland coals may be assumed to approach unity (Zhou and Ballentine, 2006), the release rate of fissiogenic ^{129}I from coals is likely quite low due to factors such as a greater atomic radius, lower diffusivity and interactions between I and the coal maceral. If, for example, ^{129}I is assumed to behave similarly to ^{222}Rn in a setting where $\varepsilon = 1$ for ^4He, the ^{129}I escape efficiency would be expected to vary from $\varepsilon = 0.03$ for grain sizes of 1μm, to something on the order of $\varepsilon = 0.0007$ when grain size exceeds 30 μm (Torgersen, 1980). Given the uncertainties, ^{129}I escape efficiencies cited in the literature vary significantly. In fine-grained, loosely consolidated marine sediments, it has been estimated that $\varepsilon = 1$ (Fehn et al., 2000). For brines associated with deep crustal fluids, estimates range from $\varepsilon = 1$ (Bottomley et al., 2002; Starinsky and Katz, 2003) to $\varepsilon = 0.15$ (Fehn et al., in press), given the assumption that porosity is 0.01. The latter of the two estimates for ε may represent a more reasonable value for coals, especially when compared to other published host rock types. When ε-values have been calculated based on ^{129}I accumulated in old groundwaters for which other constraints place bounds on the age of the water, they range from $\varepsilon = 0.003$ to $\varepsilon = 0.031$ (Fabryka-Martin et al., 1991) and roughly coincide with ε-values reported for ^{222}Rn in shaley sandstones of the same locality (Andrews et al., 1991).

In order to calculate the escape efficiency for the Fruitland Formation coals, the amount of excess ^{129}I in the porewaters was calculated, and ε-values were adjusted to yield an age identical to the coals (73 Ma) for the most concentrated water sample (I = 109μM). The initial marine-cosmogenic $^{129}I/I$ ratio (1500×10^{-15}) for I in the 73-Ma Fruitland Formation would have decayed to a ratio of 60×10^{-15} at the present-day, were there no subsequent addition of fissiogenic ^{129}I to the fluid. For an I-rich groundwater sample from this formation, it is assumed that any elevation of its $^{129}I/I$ ratio significantly above 60×10^{-15} is therefore due to accumulation of fissiogenic ^{129}I produced *in situ*. Using parameters described in Table 1 and the measured $^{129}I/I$ ratio (143×10^{-15}), for the most I-rich sample (13.84 mg/L), over half (58%) of the ^{129}I in this sample is estimated to be fissiogenic in origin. Using Eq. (2), the escape efficiency ε is about 0.006, ranging from 0.002 to 0.02 when one factors in variability in U concentrations and porosities. Compared to previously published values, this range coincides with that inferred for shaley sandstones by Fabryka-Martin et al. (1991). This range seems a reasonable balance between the generally higher diffusion rate expected for reduced I^- and other conservative anions, countered by the generally limited diffusive migration of readily sorbed organohalogen molecules out of coal micropores (Littke and Leythaeuser, 1993; Levine, 1993).

As waters remain in contact with coals over time, the concentration of dissolved stable I has a significant impact on the eventual $^{129}I/I$ ratio in the waters, as illustrated in Fig. 3. The initial values for $^{129}I/I$ ratios of both I-rich formation waters and I-poor meteoric waters is assumed to be the same as the marine-cosmogenic ratio. Over time, reconstructed ratios of $^{129}I/I$ in formation waters (FW) decrease as the marine-cosmogenic ^{129}I component decays. In contrast, $^{129}I/I$ ratios in dilute waters derived from meteoric sources (MW) are expected to increase over time due to accumulation of *in situ* produced ^{129}I in the pore fluids. These general trends are expected to be manifest even given that the parameter values used in Eq. (2) will deviate somewhat from the assumed averages due to heterogeneities within the host formation. If, for

Table 1
Parameter values used in this study

Parameter	Symbol	Value	Units	Reference
Physical constants				
^{129}I decay constant	λ_{129}	4.41×10^{-8}	y^{-1}	1
^{36}Cl decay constant	λ_{36}	2.30×10^{-6}	y^{-1}	1
Isotopic abundance of ^{35}Cl	–	75.77	%	1
^{238}U spontaneous fission yield at mass 129	Y_{129}	3×10^{-4}	Nuclei/fission	4
^{238}U spontaneous fission decay constant	λ_{sf}	8.5×10^{-17}	y^{-1}	3
Average neutron yield per spontaneous fission of ^{238}U	υ	2.0	n fis.$^{-1}$	8
Thermal-neutron-absorption cross-section of ^{35}Cl	σ	43.6×10^{-24}	cm^2	7
Formation-specific parameters				
Coal density	ρ	1.79	g cm^{-3}	9
Effective porosity	Φ	0.01	Dimensionless	6
U in coal	[U]	2.8	ppm	2
Th in coal	[Th]	7.0	ppm	2
^{129}I escape efficiency in coal	ε	0.006	Dimensionless	5
Thermal neutron flux in coal	Φ	270	n-$cm^{-2}y^{-1}$	5

[1]Parrington et al., 1996; [2]Affolter, 2000; [3]Decarvalho et al., 1982; [4]Hebeda et al., 1987; [5]This study; [6]Young et al., 1991; [7] Mughabghab et al., 1981. [8]Holden and Zucker, 1983; [9]Zhou and Ballentine, 2006.

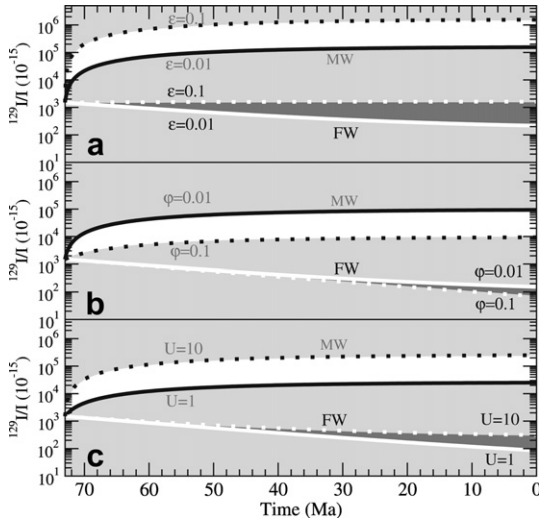

Fig. 3. Time trajectory plots for ^{129}I/I ratios for formation waters (FW, white lines, dark gray shaded region) and meteoric waters (MW, black lines, white shaded region), residing in the coals for 73 Ma. Plots showing the effect of changing individual variables in Eq. (2) while holding the others constant as in Table 1. Iodine-rich FWs show a decrease in ^{129}I/I over time, while I -poor MW waters show increasing ^{129}I/I ratios. (a) Increasing the escape efficiency of ^{129}I from 0.01 (solid line) to 0.1 (dotted line) causes an increase in ^{129}I/I by roughly an order of magnitude in present-day waters. (b) Increasing porosity by an order of magnitude causes a decrease in ^{129}I/I (dotted lines), particularly in MW. (c) Increasing U concentrations by an order of magnitude causes an increase in ^{129}I/I identical to the case for (a).

example, the estimated escape efficiency were to be increased by an order of magnitude, the response in dilute meteoric waters would be an almost immediate increase in ^{129}I/I ratio, e.g., at 70 Ma, ^{129}I/I would be about 10^{-11} for $\varepsilon = 0.01$ versus 10^{-10} for $\varepsilon = 0.1$ (Fig. 3a, black lines). Conversely, the change in I-rich formation waters initially would be negligible; at 70 Ma, the ^{129}I/I ratio would be nearly indistinguishable from its initial marine-cosmogenic value of 10^{-12} regardless of whether $\varepsilon = 0.01$ or $\varepsilon = 0.1$ (Fig. 3a, white lines). Eventually, for both water end-members, the effect of an order-of-magnitude increase in ε is an order-of-magnitude increase in the secular equilibrium ^{129}I/I ratio as well. Similarly, an order-of-magnitude increase in porosity (e.g., from 1% to 10% in Fig. 3b) results in only a small and gradual decrease in the FW ^{129}I/I ratios (white lines), while the same increase in porosity has a dramatic and immediate impact on reducing the rate of increase in ^{129}I/I ratios in MW (black lines). Finally, the responses of the end-member fluids to an order-of-magnitude increase in U content in the host rock (from 1 ppm to 10 ppm in Fig. 3c) parallel the trends for an order-of-magnitude increase in the escape efficiency for fissiogenic ^{129}I (Fig. 3a).

3.3. Anthropogenic sources of ^{129}I

Above-ground testing of nuclear devices in the 1950s and 1960s coupled with ongoing nuclear reprocessing has dramatically increased the ^{129}I inventory in surface reservoirs (e.g. Moran et al., 1999, 2002; Snyder and Fehn, 2004; Aldahan et al., 2007; Atarashi-Andoh et al., 2007; Schnabel

et al., 2007). In order to characterize the anthropogenic ^{129}I end-member in the San Juan Basin area, surface waters were collected from lakes and streams. In addition, shallow monitoring wells yielded waters from quaternary alluvium overlying the Fruitland Formation in areas near the coal outcrops (Snyder et al., 2003; Riese et al., 2005). Anthropogenic waters would be expected to have high excess ^{129}I concentrations as well as elevated ^{129}I/I ratios. Ratios for river and lake samples ranged across three orders of magnitude, from $3.9 \pm 0.9 \times 10^{-12}$ to $2.5 \pm 0.1 \times 10^{-9}$ (Snyder et al., 2003). A variety of effects probably contribute to the observed variability in the ^{129}I/I ratios for local surface waters, including varying amounts of snowmelt (Riese et al., 2005), microbial scavenging of oxidized I, adsorption, and dilution by brine seeps. In any case, meteoric waters (MW) older than 50 a (PRE-ANT) can be distinguished from younger anthropogenic meteoric waters (ANT) if the residence time in the host rock is sufficiently short so that the ^{129}I/I ratio can be assumed to be unaffected by ^{129}I decay or *in situ* production. On the other hand, the interpretation of ^{129}I/I above 1500×10^{-15} in production wells with dilute waters may be less certain, as these waters could either be old PRE-ANT affected by *in situ* production, or recently infiltrated ANT. In such a case, other techniques for bounding the residence time of dilute waters in the formation, such as ^{4}He age dating, are invaluable for distinguishing between the two meteoric I end-members. The dissolved gas data suggest that ^{4}He ages are in the tens of thousands to hundreds of thousands of years even a few km from the western outcrop for the Fruitland Formation (Zhou and Ballentine, 2006). The accumulation of ^{4}He strongly supports the hypothesis that the predominant meteoric end-member is PRE-ANT which has subsequently also accumulated ^{129}I from *in situ* sources.

3.4. Temporal trends resulting from mixing of ^{129}I sources

Assuming that the predominant component of groundwater in the Fruitland formation predates the age of nuclear testing, the obvious question is whether these waters were introduced during (or shortly after) the deposition of the peats along the shorelines of the Western Interior Seaway or, alternatively, during uplift of the basin to form the present structural hingeline. Perhaps, based on the interpretation of ^{4}He data by Zhou and Ballentine (2006), the residence time of the dilute hydrocarbon waters is even less than a million years.

Modeled time-trajectories of ^{129}I concentrations and ^{129}I/I ratios (Fig. 4) were constructed to distinguish among these alternatives, based on end-member compositions as defined in Table 2 and parameter values assumed in Table 1. Fig. 4a models the effect of adding varying proportions of low-I meteoric water (PRE-ANT) to the pre-existing I-rich formation water (FW) at 40 Ma, just prior to the formation of the structural hingeline. A mixture of 95% FW and 5% PRE-ANT starting at 40 Ma will follow a similar decay trajectory as the undiluted formation waters, and with a present-day ^{129}I concentration that is indistinguishable from that which pure FW would have at the present-day. Similarly, a mixture of 50% FW and 50% PRE-ANT starting at 40 Ma would have an ^{129}I concentration which is only modestly lower (by about 20%) than pure FW would be at present.

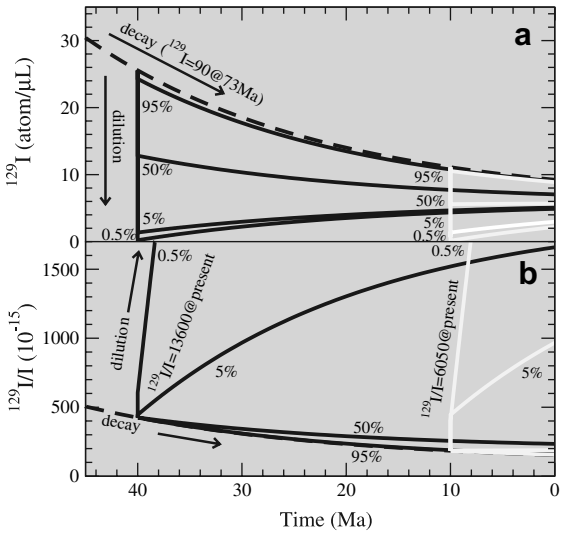

Fig. 4. Effect of dilution of formation water (FW) with varying amounts of meteoric water (PRE-ANT) at 40 Ma (black lines) and 10 Ma (white lines). Lines labeled with % FW in the mix. The black dashed line shows the combined effect of decay and *in situ* production, assuming no subsequent addition of more recent water. Trends calculated using end-member concentrations (Table 2) and combined decay of the marine-cosmogenic source (Eq. (1)) with in situ production (Eq. (2)). (a) Effect of dilution on ^{129}I concentration. FW diluted to 5% of its original I content by PRE-ANT, increases its ^{129}I content due to fissiogenic production. The accumulation of fissiogenic ^{129}I (and hence also ^{129}I/I) is greater if dilution occurs at 40 Ma rather than at 10 Ma. (b) Effect of dilution on ^{129}I/I ratios. Note that present-day ratios (at time = 0) differ depending on the extent of dilution as well as when the dilution occurred (e.g., at 40 Ma or at 10 Ma).

Table 2
Fruitland Formation starting compositions for aqueous end-members

End-member	Cl (mM)	I (μM)	$^{129}I/I_{init}$ (10^{-15})	$^{36}Cl/Cl_{init}$ (10^{-15})	$^{129}I_{init}$ (at/μL)	$^{36}Cl_{init}$ (at/μL)
Formation water (FW)[a]	223	109	1500	1.04	90.3	140
Present meteoric (ANT)[b]	0.01	0.1	2550000	1600	153	9.63
Pre-anthropogenic (PRE-ANT)[c]	0.01	0.1	1500	1600	0.903	9.63
Seawater (SW)[d]	530	0.44	1500	1	0.398	319

[a] Formation water end-member based on maximum measured I and Cl^- concentrations in production wells (Snyder et al., 2003; Riese et al., 2005). Assumed to be initially brackish mix of 42% seawater and 58% river water.
[b] Anthropogenic end-member based on maximum $^{129}I/I$ ratio measured for river water in the San Juan Basin (Snyder et al., 2003).
[c] Pre-anthropogenic end-member assumes the same Cl^- and I^- concentrations as for anthropogenic water, but with a marine-cosmogenic $^{129}I/I$ ratio (Moran et al., 1998) and present-day $^{36}Cl/Cl$ ratios in the San Juan Basin.
[d] Seawater composition based on average Cl^- and total I concentrations (Broecker and Peng, 1982), with $^{36}Cl/Cl$ assumed to be at the AMS detection limit (Sharma et al., 2000).

When the formation waters are extremely diluted with low-I PRE-ANT (95–99.5% PRE-ANT) at 40 Ma, the concentration of ^{129}I in solution actually increases over time because the ^{129}I contribution from fissiogenic production exceeds the rate of its removal by decay. A similar, although less obvious, pattern develops if meteoric recharge is assumed to have occurred in the more recent past. For example, infiltration of meteoric waters at 10 Ma shows the same trends as for infiltration at 40 Ma but, because fissiogenic ^{129}I has less time to accumulate in the dilute waters, the resulting ^{129}I concentrations are lower than for the 40-Ma dilution event.

The dilution of FW water by varying amounts of PRE-ANT in the past can also lead to significantly different outcomes for present-day $^{129}I/I$ ratios because PRE-ANT dilutes the amount of stable ^{127}I in solution while having no effect on the fissiogenic production and release of ^{129}I (Fig. 4b). As with ^{129}I concentrations, dilution by 5% PRE-ANT at 40 Ma produces negligible shifts in $^{129}I/I$ ratios, and the effect of even 50% dilution by PRE-ANT is small. Where the residual quantity of FW water in the mixture is less than 5%, however, the $^{129}I/I$ ratio can actually increase by over an order of magnitude, provided that the dilution event occurred sufficiently long ago. If dilution occurs more recently, the ratio will not increase as much. For example, a mixture of 0.5% FW and 99.5% PRE-ANT at 40 Ma will evolve to a $^{129}I/I$ ratio of 13.6×10^{-12} by modern times, while the present-day ratio will only reach 6.05×10^{-12} for a mixing event occurring at 10 Ma.

This modeled evolution of the isotopic signature of mixed water sources over time illustrates two important principles of the ^{129}I system. Firstly, if the objective is to study the organic source of a hydrocarbon system similar to the Fruitland coals, dilutions of the original I-rich formation water by 5%, or even by as much as 50%, of more recent meteoric water will only modestly affect the observed $^{129}I/I$ ratios and I isotopic "ages" calculated based on those ratios. Secondly, in dilute hydrocarbon waters, where residual formation water constitutes less than 5% by volume, the timing of the onset of mixing will measurably affect the present-day $^{129}I/I$ ratios.

The evolution of ^{129}I concentrations over time, as a function of the volumetric fraction of formation water (X_{fw}) and the timing of dilution, is illustrated in Fig. 5a. As with the model illustrated in Fig. 4, both decay and *in situ* production of ^{129}I are accounted for. For well and surface waters considered in this paper, the fraction of formation water in each was estimated by dividing the measured I concentration by the highest concentration observed in the coal formation water (109 μM). It is possible that higher dissolved I concentrations exist within coalbed waters but were not among the sampled locations. Assuming that the I end-member may be underestimated, the fractions of formation water calculated by this approach are likely maximum estimates. For the sake of simplicity, the trend lines assume two-component mixing of PRE-ANT and FW. Measured values for surface waters and some monitoring wells plot above the trend-lines and along the right-hand axis due to the presence of anthropogenic additions. Nonetheless, many of the production wells do fall within the trend lines. For those samples in which the proportion of formation water (X_{fw}) is less than 20%, dilution with pre-anthropogenic meteoric water generally appears to have occurred much more recently than 10 Ma (Fig. 5a), a trend that is also supported

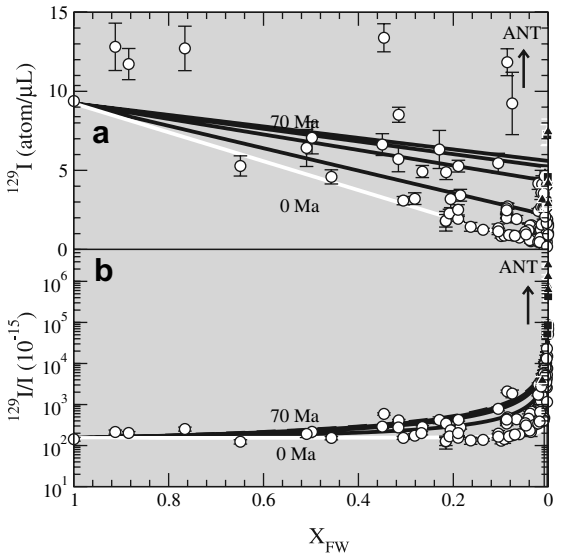

Fig. 5. Modeled effect of mixing different proportions of formation water with meteoric water at different times in the past. Arrow labeled ANT indicates that mixing with recent anthropogenic water shifts ^{129}I values above the modeled trend lines. Open circles = production well values, Closed squares = shallow monitoring wells, Closed triangles = rivers and streams.

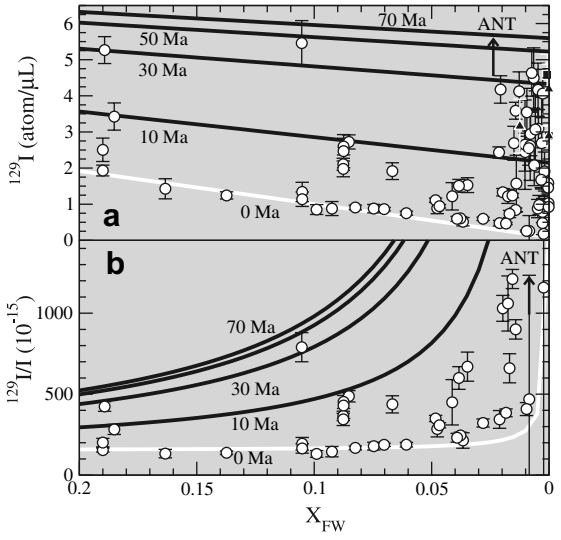

Fig. 6. Expanded plot, as in Fig. 5, showing I isotopic composition where the fraction of initial formation water is less than 20%. The plotting location for most of the dilute samples is consistent with a mixing event occurring sometime between the present and 10 Ma.

by examination of the observed ^{129}I/I ratios (Fig. 5b). An expanded view for these samples (Fig. 6) shows the trend more clearly, and indicates that, for these waters at least, the end-member and production parameters in Tables 1 and 2 appear to be reasonable. However, when the proportion of residual formation water (X_{fw}) drops below 0.05, it becomes increasingly difficult to distinguish based on the ^{129}I data alone, whether the waters have residence times in the tens of millions of years, or whether a component of anthropogenic meteoric water may be present.

4. ^{36}Cl sources in coalbed systems

4.1. ^{36}Cl derived from the atmosphere

In order to assess the input of groundwater less than several Ma, a subset of production wells in the Fruitland Formation and surface waters in the San Juan Basin were analyzed for ^{36}Cl (Snyder et al., 2003; Riese et al., 2005). These data provide further information on mixing of end-member waters within the coals because the half-life of ^{36}Cl is much shorter (301 ka) than that of ^{129}I such that very old waters (>1 Ma) in the basin may be assumed to have ^{36}Cl derived entirely from *in situ* production.

In areas near the outcrop of the Fruitland Formation, most water collected from the monitoring wells derives from recharge of fresh water with its content of stable Cl and ^{36}Cl washed out of, or deposited from, the atmosphere. The predominant sources of atmospheric ^{36}Cl are spallation of ^{40}Ar in the stratosphere (Scheffel et al., 1999), and neutron-capture by ^{36}Ar in the troposphere (Andrews et al., 1986). The residence time of ^{36}Cl in the stratosphere is 2 a (Synal et al., 1990). As ^{36}Cl is transferred across the tropopause, the residence time is reduced to only a few weeks in the troposphere (Scheffel et al., 1999; Rao et al., 2005), from which it is quickly removed by precipitation and dry fallout. Production rates vary by latitude, and seasonal fluctuations control the location and rate of transfer of ^{36}Cl between the stratosphere and troposphere (Synal et al., 1990; Scheffel et al., 1999).

Deposition of atmospheric ^{36}Cl over the oceans has no detectable effect on seawater ^{36}Cl/Cl ratios. A global mean deposition rate of 24 atoms ^{36}Cl/m^2 s (Scheffel et al., 1999), distributed over 3.6×10^8 km^2 of ocean (Lisitzin, 1996), with a mean life for ^{36}Cl of 434 ka ($t_{1/2}$/ln 2) yields a steady-state marine-cosmogenic reservoir of 2.0×10^3 mol. Considering that the total stable Cl^- reservoir in the oceans is on the order of 7.4×10^{20} mol (550 mM

Cl, Broecker and Peng, 1982; 137×10^9 km^3 ocean, Lisitzin, 1996), the average ^{36}Cl/Cl ratio in seawater is 2.7×10^{-18}. This ratio is several orders of magnitude below the ^{36}Cl/Cl detection limit of AMS (10^{-15}, Sharma et al., 2000). The cosmogenic flux of ^{36}Cl in rainfall and in freshwater bodies is readily detectable, however, because of the low background of stable Cl^- in meteoric waters (usually $\ll$1 mM).

On land, the predominant source of stable Cl^- in rain water is from marine aerosols. Because the seaspray component decreases systematically with increasing distance from the ocean, observed ratios of ^{36}Cl/Cl from shallow wells and springs show a corresponding increase with increasing distance from coastlines (Davis et al., 1998, 2000, 2001). Based on the highest observed values in surface waters and monitoring wells in the San Juan Basin, the meteoric end-member is assumed to have a ^{36}Cl/Cl of 1600×10^{-15} (Snyder et al., 2003; Riese et al., 2005). Although greater than observed in most localities in the United States, this value is consistent with regional trends across the country (Davis et al., 2001).

Anthropogenic ^{36}Cl was produced in large quantities during testing of nuclear devices on ships and small islands between 1952 and 1964, as a result of neutron-capture by ^{35}Cl in seaspray and seawater. Significant proportions of this "bomb-pulse ^{36}Cl" were injected into the stratosphere by the nuclear blasts, and subsequently distributed around the globe. This bomb pulse is readily observable in ice cores from polar regions (Elmore et al., 1982; Delmas et al., 2004). These studies also show that, in contrast with ^{129}I/I ratios that continue to increase due to releases from nuclear reprocessing facilities, ^{36}Cl/Cl values in precipitation largely returned to pre-anthropogenic levels as early as the 1970s. The bomb pulse has also been observed in numerous groundwater studies (e.g., Bentley et al., 1982) and has become a widely-accepted method for detecting the presence of modern (post-bomb) water.

An inverse correlation between ^{36}Cl/Cl ratios and Cl^- concentrations for samples from surface water, monitoring wells and production wells in the San Juan Basin indicates that the presence of old saline waters exerts a dominating influence on Cl isotopic signatures in these waters. To model the temporal evolution of production waters in the Fruitland Formation, both meteoric end-members (PRE-ANT and ANT) are assumed to have the same ^{36}Cl concentrations and ^{36}Cl/Cl ratios (Table 2). Although monitoring wells and surface water samples show anthropogenic ^{129}I/I values coupled with elevated ^{36}Cl/Cl as a clear indicator of recent meteoric input, bomb-pulse ^{36}Cl is not observed in the production wells completed in the coals. The only exception to the usual co-occurrence of bomb-pulse ^{36}Cl and ^{129}I is a sample from the Florida River, that shows a high bomb-pulse ^{36}Cl/Cl ratio coupled with a pre-anthropogenic ^{129}I/I ratio. Such an apparent discrepancy could easily be explained as a consequence of mixing of river water with discharge of pre-anthropogenic water from a spring (Snyder et al., 2003; Riese et al., 2005).

4.2. ^{36}Cl production in rocks and sediment

In addition to ^{36}Cl atmospheric input into groundwater systems, ^{36}Cl is produced in shallow sediments and rocks through cosmic ray interactions, principally spallation reactions of ^{39}K and ^{40}Ca, as well as cosmogenic thermal neutron activation of ^{35}Cl. These production mechanisms form the basis for surface exposure dating methods using ^{36}Cl (e.g. Phillips et al., 1990; Zreda et al., 1993; Zreda and Noller, 1998). However, the cosmogenic influence attenuates rapidly (Andrews et al., 1991), such that at depths greater than 3 m the predominant form of *in situ* ^{36}Cl production is through the reaction $^{35}\mathrm{Cl}(n,\gamma)^{36}\mathrm{Cl}$. The neutrons in this case are those emitted during spontaneous fission of ^{238}U as well as those produced by (α,n) reactions with light nuclei, for which the sources of α-particles are the U and Th α-decay series. A major inventory of ^{35}Cl in subsurface rocks resides in their pore fluids. As such, the distribution of *in situ* produced ^{36}Cl in old groundwaters differs from a number of other *in situ* radionuclides, including ^{129}I, in that it is produced in the aqueous phase at the same rate (when normalized to total Cl) as it is produced in the rock matrix (Lehmann and Purtschert, 1997).

This important and unique characteristic of ^{36}Cl is more obvious when one examines the equation used to predict its steady-state concentration. The steady-state concentration of *in situ* produced ^{36}Cl is calculated as follows (Andrews et al., 1986):

$$N_{36} = N_{35}\sigma\Phi(1 - e^{-\lambda_{36}t})/\lambda_{36}, \quad (4a)$$

which can be re-arranged to show that the steady-state ratio is independent of Cl^- concentration:

$$N_{36}/N_{35} = \sigma\Phi(1 - e^{-\lambda_{36}t})/\lambda_{36}. \quad (4b)$$

In this case, N_{35} = concentration of ^{35}Cl in solution (75.77% of the total Cl^- concentration; the remaining 24.23% is ^{37}Cl, which does not participate in the reaction). The thermal-neutron absorption cross section for ^{35}Cl, $\sigma = 43.6 \times 10^{-24}$ cm^2, and the decay constant for ^{36}Cl, $\lambda_{36} = 2.3 \times 10^{-6}$ a (Parrington et al., 1996). Finally, the thermal neutron flux (Φ), in n/cm^2 a, can be estimated from the elemental composition of the host formation rocks (Andrews et al., 1986). Analogous to steady-state radionuclide concentrations, the neutron flux is determined by the balance between the rate at which neutrons are produced in the rock against the rate at which these neutrons are subsequently attenuated and ultimately absorbed by nuclei in that environment:

$$\Phi = P_n/\sigma_m, \quad (5)$$

where P_n is the neutron production rate (n g^{-1} a^{-1}) and $\sigma_m$is the rock's macro-absorption cross-section for thermal neutrons (cm^2 g^{-1}). The inverse of σ_m, when multiplied by the rock density (g cm^{-3}), is the mean neutron pathlength in the rock and is typically on the order of a few tens of centimeters.

In order to assess the *in situ* production of ^{36}Cl within the Fruitland coals, the thermal neutron flux is estimated from elemental data on whole-coal composition for the Fruitland Formation. The neutron production rate (P_n) may be expressed as (Andrews et al., 1989):

$$P_n = \lambda_{sf} \upsilon [U] + a[U] + b[Th], \quad (6)$$

where the first term is production of neutrons through spontaneous fission of ^{238}U, and the last two terms are production from (α, n) reactions. As with Eq. (2), λ_{sf} is the decay constant for ^{238}U spontaneous fission (8.5×10^{-17} a^{-1}, Decarvalho et al., 1982). The average neutron yield per spontaneous fission of ^{238}U (υ) is 2.0 n/fission (Holden and Zucker, 1983), and coefficients a and b are neutron yield factors that are a function of the elemental composition of the rock matrix (Table 3). In the case of the Fruitland coals,

Table 3
Calculated neutron production rate from (α, n) reactions in the Fruitland Formation

Element *i*	Mass Stopping Power[a]	n/yr/g *i* per[b]		Sample ppm[c]	Weight factor[d]	n/yr/g rock per[e]	
		ppm U	ppm Th			ppm U	ppm Th
Li	548	23.860	10.540	20	0.011	0.26	0.12
B	527	62.551	19.779	89	0.047	2.93	0.93
Be	529	265.948	91.561	0.97	0.001	0.14	0.05
C	561	0.455	0.179	591000	331.551	150.97	59.25
N	550	1.920	1.103	13000	7.15	13.73	7.89
O	527	0.236	0.084	296700	156.361	36.85	13.08
F	472	41.330	16.362	65	0.031	1.27	0.50
Na	456	12.535	5.959	2100	0.958	12.00	5.71
Mg	461	5.834	2.564	1000	0.461	2.69	1.18
Al	444	5.116	2.585	24000	10.656	54.52	27.55
Si	454	0.690	0.339	49000	22.246	15.35	7.54
P	433	4.473	0.573	150	0.065	0.29	0.04
S	439	0.103	0.173	9000	3.95	0.41	0.68
Cl	431	1.297	0.793	95	0.04	0.05	0.03
K	414	0.89	0.08	780	0.323	0.29	0.03
Ca	428	0.282	0.026	7800	3.338	0.94	0.09
Fe	351	0.187	0.208	5200	1.825	0.34	0.38
			Total	1000000	539	293	125

The factor a in Eq. (6) is calculated as the ratio of the total neutron yield per gram per ppm U, to the total weight factor, i.e., $a = 293/539 = 0.54$. The factor b is calculated similarly for Th:$b = 125/539 = 0.23$.

[a] Mass stopping power for α-particles with an initial energy of 8.0 MeV, with units MeV/(g/cm^2) (Ziegler, 1977).

[b] Elemental neutron yields from Heaton et al. (1988, 1990) and Heaton (personal communication).

[c] Average composition of Fruitland coal from Affolter (2000, Tables A1-13 and A2-13) and the National Coal Resources Data System (2006), except for O, which was set at the value needed for the total concentration to sum to 1 000 000 ppm.

[d] Weight factor is calculated by multiplying the sample's fractional concentration of each element (ppm $\times 10^{-6}$) by that element's mass stopping power.

[e] Neutron yield per gram of rock per ppm U is calculated by multiplying each element's weight factor by the neutron yield for that element per ppm U. The neutron yield per gram of rock per ppm Th is calculated by the same approach.

$$P_n = 0.43[U] + 0.54[U] + 0.23[Th], \quad (7)$$

where U and Th concentrations are in ppm, and the numerical coefficients have units of n g^{-1} a^{-1} ppm^{-1}. Assuming a basinwide average of U = 2.8 ppm and Th = 7.0 ppm (Affolter, 2000, Table A2-13) yields $P_n = 4.3$ n g^{-1} a^{-1}. Atypical of most geologic formations, (α, n) reactions with C nuclei account for a large fraction (about 32%) of the *in situ* neutron production rate in the Fruitland Formation (Table 3); more commonly, the contribution of neutrons from (α, n) reactions with C nuclei is negligible due to the relatively low C concentration in most rocks.

The production of ^{36}Cl from the $^{35}Cl(n,\gamma)^{36}Cl$ reaction is not only a function of the rate of neutron production in the formation, but also the rate at which those neutrons are thermalized and attenuated by other elements that compete in neutron scattering and absorption and that control the neutron energy spectra and the distance over which the *in situ* thermal neutron flux attenuates. Using average elemental concentrations for the Fruitland Formation coals from Affolter (2000) and National Coal Resources Data System (2006), the macro-absorption cross-section for thermal neutrons is 1.59×10^{-2} g/cm^2 (Table 4). The resulting thermal-neutron flux is 270 n cm^{-2} a^{-1}, and corresponds to a low secular equilibrium $^{36}Cl/Cl$ of 4×10^{-15}. Because the neutron yield per ppm C is considerably less than the yields for Si and Al (Table 3), this estimated neutron flux for Fruitland coals is less than fluxes calculated for other sedimentary rocks, such as those in the Milk River aquifer (shale $\Phi =$ 331 n/cm^2/a; sandstone $\Phi = 674$ n/cm^2/a; Andrews et al., 1991), and in the Great Artesian Basin (shale $\Phi = 915$ n/cm^2/a; sandstone $\Phi = 410$ n/cm^2/a; Lehmann et al., 2003). Nonetheless, the validity of the approach is indicated by the observation that, in both of these groundwater studies, measured $^{36}Cl/Cl$ ratios in the distal portions of the flow systems matched those predicted from the calculated neutron fluxes.

Table 4
Calculated macro-absorption cross-section for Fruitland Formation coal

Z		Atomic weight	Thermal neutron absorption cross-section[a] (10^{24} cm^2)	Element concentration[b] (ppm)	Macro-absorption thermal neutron cross section[c] (10^6 cm^2/g rock)
1	H	1.0	0.333	51 000	10 144
3	Li	6.9	71	20	123
5	B	10.8	764	89	3787
6	C	12.0	0.0035	591 000	104
7	N	14.0	0.0747	13 000	42
8	O	16.0	0.00028	244 548	3
9	F	19	0.0094	65	0
11	Na	23.0	0.53	2100	29
12	Mg	24.3	0.066	1000	2
13	Al	27.0	0.23	24 000	123
14	Si	28.1	0.168	49 000	176
15	P	30.97	0.17	150	0
16	S	32.07	0.516	9000	87
17	Cl	35.453	33.5	95	54
19	K	39.1	2.1	780	25
20	Ca	40.1	0.43	7800	50
22	Ti	47.88	6.1	1100	84
25	Mn	54.9	13.3	45	7
26	Fe	55.8	2.56	5200	144
62	Sm	150.4	5600	2.9	65
64	Gd	157.3	49 000	4.8	900
				1 000 000	15 949

[a] Cross-sections from Parrington et al. (1996).

[b] Average composition of Fruitland coal from Affolter (2000, Tables A1-13 and A2-13) and the National Coal Resources Data System (2006), except for O, which was set at the value needed for the total concentration to sum to 1 000 000 ppm.

[c] Each element's contribution to the rock's macro-absorption cross-section is calculated as the product of its atomic density in the rock and its absorption cross-section for thermal neutrons. These contributions are then summed to obtain the rock's total macro-absorption cross-section (i.e., 0.0159 cm^2/g in this case).

4.3. Temporal trends resulting from mixing of formation and meteoric waters

If the predominant Cl^- source in waters of the Fruitland Formation were to have a minimum residence time of about 2 Ma, then the $^{36}Cl/Cl$ ratio would have attained secular equilibrium with the neutron flux of the coals. Modeled time trajectories in Fig. 7a shows the effect of diluting formation waters at an arbitrary point in time (5 Ma), using end-member concentrations and $^{36}Cl/Cl$ ratios defined in Table 2 and the neutron flux estimated in the previous section. The effect of dilution by meteoric water on ^{36}Cl concentrations is quite different than its effect on ^{129}I. Because dilution effectively reduces the concentration of stable ^{35}Cl available to undergo (n,γ) reactions, secular equilibrium concentrations for different degrees of dilution never converge, although equilibrium $^{36}Cl/Cl$ ratios do. In contrast, *in situ* production over tens of millions of years produces converging ^{129}I concentrations (Fig. 4a). Secular equilibrium ^{36}Cl concentrations and $^{36}Cl/Cl$ ratios are established after approximately 2 Ma (Figs. 7 and 8). Even if Cl^--rich waters were to enter the coalbeds from some other external source, for example inter-formational flow of brine

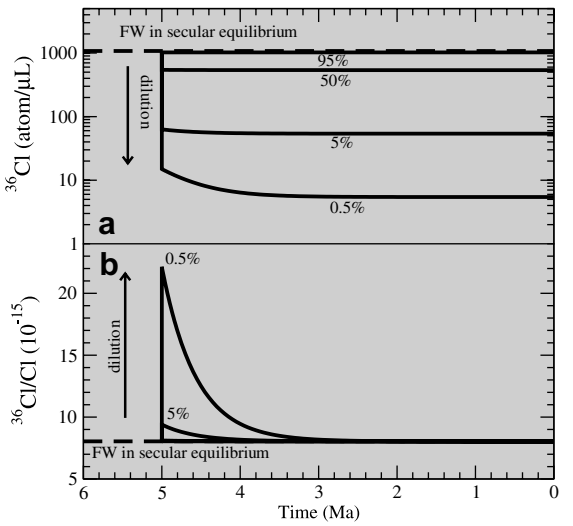

Fig. 7. Model plots showing the effect of instantaneous dilution of Cl^--rich formation waters by meteoric water at 5 Ma. Older FW water in secular equilibrium with respect to ^{36}Cl in the coals is indicated by the dashed line. (a) New secular equilibrium values for ^{36}Cl are reestablished as a function of the stable Cl^- content. (b) Effect of dilution on $^{36}Cl/Cl$ ratios. The initial peak ratio at the time of mixing with meteoric water is only detectable in waters containing less than 5% of the FW component, and decays back to secular equilibrium values within 2 Ma or less.

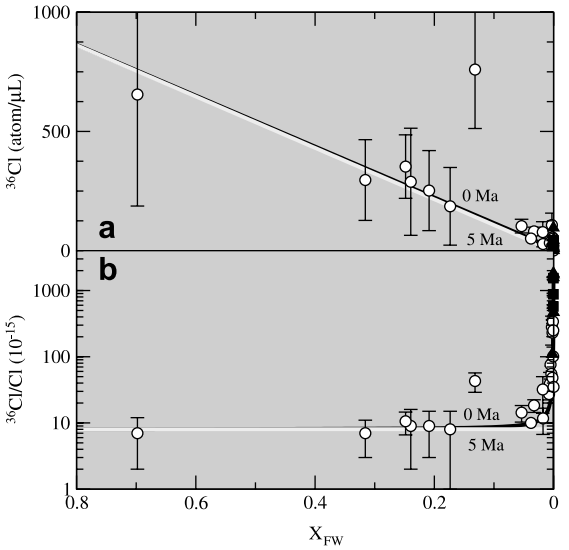

Fig. 8. Modeled ^{36}Cl composition as a function of the fraction of Cl^- derived from FW at 5 Ma (white line) and at the present (black line). (a) Secular equilibrium values for ^{36}Cl decrease with increasing dilution (i.e., lower X_{fw} values). Only one sample shows possible admixture of bomb-pulse ^{36}Cl with FW. (b) Because secular equilibrium values of ^{36}Cl are directly proportional to stable Cl concentrations, $^{36}Cl/Cl$ ratios do not change appreciably.

from a more uraniferous deeper layer below the Fruitland Formation, local secular equilibrium values would still be re-established within a couple of million years.

Fig. 7b also illustrates that the presence of even seemingly minor amounts of formation water will dramatically decrease the elevated $^{36}Cl/Cl$ ratios that are characteristic of meteoric waters. For example, the presence of only 0.5% formation water reduces the $^{36}Cl/Cl$ ratio from 1600×10^{-15} (representing local surface waters) to less than 25×10^{-15} in the mixture. This sensitivity is further illustrated over a broad range of mixing ratios (Fig. 8) as well as an expanded plot showing the effect of the presence of 2% or less of saline formation water in a system that is otherwise derived from meteoric sources (Fig. 9). The Cl^- fraction, X_{fw} was calculated from the ratio of measured and end-member Cl^- concentrations. As has been discussed by previous investigators (e.g. Davis et al., 2000), this sensitivity often complicates attempts to trace the migration of meteoric waters through aquifer systems based on ^{36}Cl age-dating of the input source (Davis et al., 2000).

The ^{36}Cl concentrations and $^{36}Cl/Cl$ ratios measured for the production wells coincide with the *in situ* secular equilibrium values calculated from

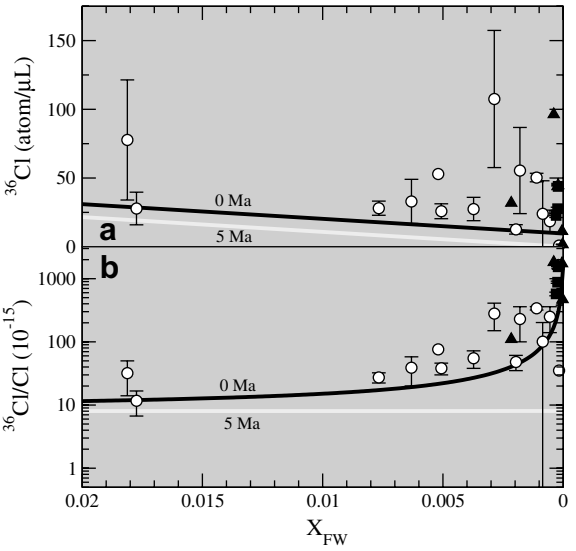

Fig. 9. Expanded plot, as in Fig. 8, illustrating trends where the percentage of FW in the groundwater drops to less than 2%. (a) Very dilute samples show slight excess amounts of ^{36}Cl. (b) None of the dilute samples show secular equilibrium values (5 Ma) for ^{36}Cl, suggesting that mixing occurred at less than 2 Ma.

Eq. (4b) (Fig. 9). Deviations between trends predicted for old mixing and recent mixing (Fig. 8) are less obvious than those observed with ^{129}I. Discernible differences only arise for the case in which mixing occurred more recently than 2 Ma, and the remaining formation water is less than 1% (Fig. 9). Of the production-well samples for which $X_{fw} < 0.01$, none appear to have attained secular equilibrium with respect to ^{36}Cl, as illustrated by their position well above the trendline for mixing occurring at 5 Ma. This disequilibria supports the hypothesis that mixing occurred in recent (<2 Ma) times for these waters.

Combination of the ^{129}I and ^{36}Cl systems elucidates the nature of the mixing trends affecting dilute groundwaters (Fig. 10). For waters older than 2 Ma, ^{36}Cl/Cl ratios are indistinguishable from secular equilibrium values, while the ^{129}I/I ratios are generally less than 500×10^{-15}, depending on the proportion of formation water present. A subset of points with low ^{129}I/I ratios plots roughly along the 0 Ma line, which supports the interpretation that meteoric water mixed with formation waters at some time before 50 a ago (i.e., no anthropogenic component is present), but much less than 1 Ma. The points in this second group plot slightly under the 0 Ma mixing line (and perhaps shifted slightly to the left, in terms of ^{36}Cl/Cl ratios). This shift is also seen in points plotting slightly above the 0 Ma mixing line in Fig. 9b, and may be due to the fact that the assumed pre-anthropogenic ^{36}Cl/Cl ratio for the pre-anthropogenic end-member could be underestimated. Finally, a third large subset consists of points which do not fall on any of the trajectories and have high ^{129}I/I ratios that most likely reflect the presence of anthropogenic ^{129}I.

It is worth noting that the abundance of wells in each of the three subsets is not representative of the overall density of wells in the Fruitland,

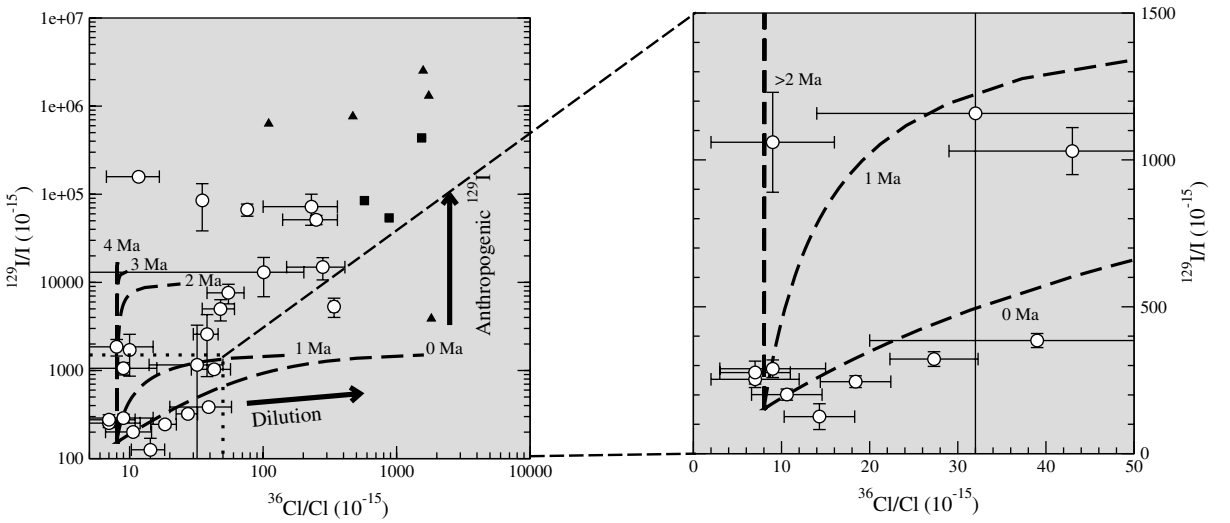

Fig. 10. Dilution more recently than 5 Ma has a combined effect on ^{129}I/I ratios and ^{36}Cl/Cl ratios. Although "ages" derived from both of these isotopic systems in dilute waters may not coincide, modeled mixing trajectories show consistent values in the waters with low ^{129}I/I ratios. Points that fall above the mixing trajectories indicate addition of anthropogenic waters younger than 50 a.

because dilute waters near the formation's outcrop were intentionally selected for ^{36}Cl studies. Nonetheless, the trends do show how a combined approach can clearly distinguish mixing between mixing of formation waters with either recent pre-anthropogenic or anthropogenic waters. Because present-day $^{36}Cl/Cl$ ratios are indistinguishable from pre-anthropogenic ratios, data for the monitoring wells and surface waters all plot above the mixing lines for waters younger than 4 Ma in

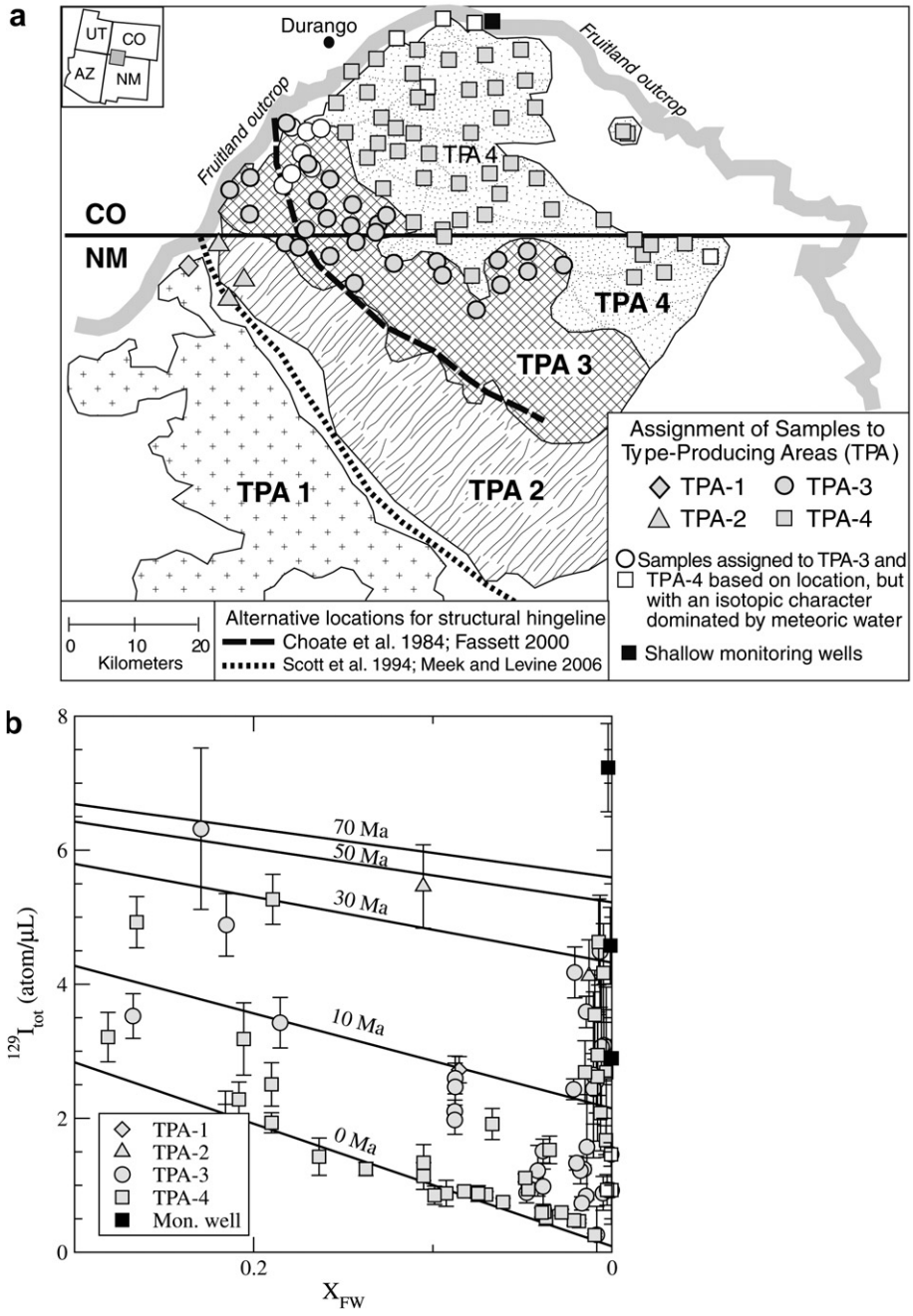

Fig. 11. (a) Map of Type Producing Areas (TPA) (modified from Meek and Levine, 2006) and wells sampled in this study. (b) Distribution of ^{129}I concentrations by Type Producing Area, plotted against mixing fraction. As with Figs. 5 and 6, mixing lines show the effect of diluting the formation water with meteoric water at 70 Ma, 50 Ma, 30 Ma, 10 Ma and 0 Ma.

Fig. 10, but not to the right of the 0 Ma mixing line. Varying contributions of anthropogenic waters in this figure therefore produce a vertical shift in ^{129}I, but do not show any horizontal shift in $^{36}Cl/Cl$. The production well data that do not fall on the mixing trajectories must also have an anthropogenic $^{129}I/I$ component, because horizontal shifts in $^{36}Cl/Cl$ would not cause them to fall within the predicted mixing trajectories.

5. Iodine isotopic signatures and well production history

The Fruitland Formation coals may be subdivided into subregions based on production histories as well as the compositions of the fluids recovered (Meek and Levine, 2006). Because one expects reservoir characteristics to be controlled largely by hydrologic characteristics such as pore connectivity, rates of flushing, and water residence times, it is logical to look for correlations not only between the ^{129}I distributions and geologic structures in the basin, but also between ^{129}I and gas compositions and production characteristics. Within the study area, Fig. 11a delineates four broadly-defined production areas based on consistency in reservoir characteristics and distinctive production behaviors (Meek and Levine, 2006). These "Type Producing Areas" (TPAs) are geographically delimited roughly in the same NW-SE direction as paleoshorelines (Fassett, 2000) and preexisting basement linears (Riese et al., 2005).

- TPA-1, SW of the study area, consists of wells with moderate to low cumulative production of fluids with moderate gas to water ratios ($G/W > 20$) (Meek and Levine, 2006).
- TPA-2 has significantly higher gas to water ratios ($G/W > 200$) and low CO_2 (Meek and Levine, 2006). TPA-2 wells have very low cumulative gas production, most produce some oil, and many produce no water. The area is bounded by two basement linears, each of which has been interpreted to coincide with the structural hingeline of the basin. The northernmost proposed location of the hingeline extends to the western outcrop of the Fruitland just above the state line (Choate et al., 1984; Fassett, 2000), and the southernmost proposed location of the hingeline extends to the western outcrop of the Fruitland at the NM-CO state line (Scott et al., 1994; Meek and Levine, 2006).
- TPA-3 wells comprise the high-production "Fairway" located to the north of the northernmost proposed location of the hingeline. TPA-3 wells have very high cumulative gas production, G/W between 20 and 200, >10% CO_2, and high peak gas-producing rates (Meek and Levine, 2006).
- Finally, TPA-4 wells have moderate cumulative gas production, and very low gas/water ratios (<20) (Meek and Levine, 2006).

In the relatively few samples that have been collected from TPA-1 and TPA-2 for the present study, none of which is >15 km from the western outcrop, these two areas generally have ⩽10% residual formation waters and show the presence of meteoric water young enough to contain anthropogenic I. Iodine concentrations in TPA-3 are variable. The lowest I concentrations, in samples dominated by meteoric water and containing <3% residual formation water (Fig. 10) are downgradient of the western Fruitland outcrop, near the hingeline of Choate et al., 1984. Many of the points for TPA-3 further away from the outcrop have 10–30% residual formation water and are clustered between the 0 Ma and 10 Ma mixing lines. None of them, however, fall directly on the 0 Ma line, suggesting that deep within the Fruitland flow system, dilution of the formation water with meteoric water occurred millions of years ago. A large proportion of the TPA-4 samples, however, plot either vertically along the meteoric water axis, indicating infiltration of young meteoric water with anthropogenic isotopes, or they plot along the 0 Ma mixing line, indicating that formation waters were diluted by a meteoric water component at some time before anthropogenic production of ^{129}I, but still on a scale that could range from as recently as 50 a ago, but equally possible, as distant in the past as a few million years ago.

6. Concluding remarks

Much of the debate surrounding interpretation of ^{129}I and ^{36}Cl data in dilute basin waters can be traced to uncertainties about the sources of, and mixing between, potential end-members. Nonetheless, the interpreted behavior of the hydrologic system must be consistent with these data, along with other chemical and isotopic considerations. If the Fruitland Formation can be considered as a representative case study, then a number of generalizations can be made regarding dilute waters, particularly in hydrocarbon systems:

1. In theory, formation waters should have $^{129}I/I$ ages that, after accounting for contributions from *in situ* production, are similar to the age of the source of organic matter with which the water is, or has been, in contact. In the case of coalbed methane systems, the relevant ^{129}I-based age is likely that of the coals themselves. Minor dilution by pre-anthropogenic water (<5%vol.) does not significantly shift $^{129}I/I$ ratios of the I-rich formation waters, and even dilutions by up to 50%vol. in the past will yield approximately the same present $^{129}I/I$ ratio.
2. Extremely dilute waters that contain less than 5%vol. of the original formation water may actually show an increase in $^{129}I/I$ ratios and ^{129}I concentrations over time due to fissiogenic production. By modeling the ingrowth of fissiogenic ^{129}I as a function of time and using site-specific parameter values, one can approximate, or at least bound, the onset of dilution. In the case of the Fruitland Formation, groundwaters affected by extensive dilution by meteoric water show that this mixing most likely occurred within the past 10 Ma. This interpretation is consistent with that based on ^{4}He data obtained from samples along the Western margin of the basin, in the area denominated by the Fairway (Zhou and Ballentine, 2006).
3. Where the fraction of residual formation water in the coals is less than 1%vol., $^{36}Cl/Cl$ ratios clearly indicate that dilution has occurred recently and does not represent compartmentalization of syndepositional features such as paleo-stream channels in the coal-forming peats. Waters in contact with the coals for over 2 Ma all show secular equilibrium concentrations of ^{36}Cl as well as $^{36}Cl/Cl$ ratios. Only one sample deviates significantly from these two trends, perhaps as the result of the presence of bomb-pulse ^{36}Cl.
4. Where $^{129}I/I$ ratios are much greater than the corresponding pre-anthropogenic $^{36}Cl/Cl$ ratios, the groundwater most likely contains ^{129}I from anthropogenic sources, indicating a component of the groundwater has a residence time less than 50 a. In general, these samples also contain less than 5% of the original formation water component, and are situated just south of the NM–CO state line where coalbeds show thinning and fracturing (Riese et al., 2005) or along the areas of formation outcrop.
5. Stratigraphic pinchouts and discontinuities between the coalbeds appear to be the major factors in isolating waters in the TPA-4 region from TPA-3, to a greater extent than regional structural features such as the presence of a basin hingeline (Meek and Levine, 2006; Riese et al., 2005). The recent interpretation of the data suggests that infiltration of paleowaters into TPA-4, more recently than a couple of Ma, was much more pervasive than in TPA-3. TPA-3 still has areas of recent recharge, but these appear to be limited to an area near the western outcrop of the Fruitland Formation.

This paper presents a fairly simple mixing model which does not contemplate all possible factors influencing ^{129}I and ^{36}Cl signatures in dilute formation waters. The possible role of the influx of fresh water on enhancing microbial degradation of organic matter and the release of I is one area that merits investigation. Nonetheless, the assumption that I is released from the peat deposits into interstitial waters during the early stages of diagenesis to form coal seems to be reasonably valid insomuch as the observed values matched reasonably with the modeled trajectory curves. The effect of extensive migration of brines from sources with vastly different lithologies into present-day traps has also not been discussed. Despite these caveats, this approach to interpretation of the Fruitland isotopic data provides a framework for determining time-series interactions of saline and fresh waters in other localities. By extension, this approach may also be applicable to evaluating the extent to which portions of large basins are subject to active throughflow, or whether they are relatively static. Further work should be carried out to test to what degree the ^{129}I system is coupled to that of the noble gases as well as to stable isotope systems that are influenced by both microbial and thermogenic gas production.

Acknowledgements

Both ^{129}I and ^{36}Cl determinations were funded by Vastar Resources as part of the 3M Project. Sample preparation was carried out at the Cosmogenic Isotope Laboratory, University of Rochester, and analyzed at the AMS facilities of PRIME Laboratory, Purdue University. G.S. gratefully acknowledges the support and suggestions provided by Udo Fehn (Univ. Rochester) at that time, as well

as ongoing discussions with Rusty Riese (BP America). Useful comments leading to the improvement of this paper were provided by Don Hickmott, L. DeWayne Cecil and Zheng Zhou.

References

3M Project, 2000. San Juan Basin, Colorado and New Mexico: Hydrologic Modeling Final Report. Applied Hydrology Associated (Eds.), Prepared for the Southern Ute Indian Tribe, Colorado Oil and Gas Conservation Commission, US Bureau of Land Management. Available from: <http://oil-gas.state.co.us/Library/sanjuanbasin/3m_project/3MCBMReport.htm>.

Affolter, R.H., 2000. Quality characterization of Cretaceous coal from the Colorado Plateau coal assessment area. In: Kirschbaum, M.A., Roberts, L.N.R., Biewick, L.R.H. (Eds.), Geologic Assessment of Coal in the Colorado Plateau: Arizona, Colorado, New Mexico, and Utah. US Geol. Surv. Prof. Pap. 1625-B (Chapter G). Available from: <http://geology.cr.usgs.gov/energy/coal/PP1625B/>.

Aldahan, A., Alfimov, V., Possnert, G., 2007. ^{129}I anthropogenic budget: Major sources and sinks. Appl. Geochem. 22, 606–618.

Amachi, S., Kamagata, Y., Kanagawa, T., Muramatsu, Y., 2001. Bacteria mediate methylation of iodine in marine and terrestrial environments. Appl. Environ. Microbiol. 67, 2718–2722.

Andrews, J.N., Fontes, J.C., Michelot, J.L., Elmore, D., 1986. *In situ* neutron flux, ^{36}Cl production and groundwater evolution in crystalline rocks at Stripa, Sweden. Earth Planet. Sci. Lett. 77, 49–58.

Andrews, J.N., Davis, S.N., Fabryka-Martin, J., Fontes, J-Ch., Lehmann, B.E., Loosli, H., Michelot, J-L., Moser, H., Smith, B., Wolf, M., 1989. The *in situ* production of radioisotopes in rock matrices with particular reference to the Stripa granite. Geochim. Cosmochim. Acta 53, 1803–1815.

Andrews, J.N., Florkowski, T., Lehmann, B.E., Loosli, H.H., 1991. Underground production of radionuclides in the Milk River aquifer, Alberta, Canada. Appl. Geochem. 6, 425–434.

Anschutz, P., Sundby, B., Lefrançois, L., Luther III, G.W., Mucci, A., 2000. Interactions between metal oxides and species of nitrogen and iodine in bioturbated marine sediments. Geochim. Cosmochim. Acta 64, 2751–2763.

Atarashi-Andoh, M., Schnabel, C., Cook, G., MacKenzie, A.B., Dougans, A., Ellam, R.M., Freeman, S., Maden, C., Olive, V., Synal, H.-A., Xu, S., 2007. ^{129}I/^{127}I ratios in surface waters of the English Lake District. Appl. Geochem. 22, 628–636.

Bentley, H.W., Phillips, F.M., Davis, S.N., Gifford, S., Elmore, D., Tubbs, L.E., Gove, H.E., 1982. Thermonuclear Cl-36 pulse in natural water. Nature 300, 737–740.

Bentley, H.W., Phillips, F.M., Davis, S.N., Habermehl, M.A., Airey, P.L., Calf, G.E., Elmore, D., Gove, H.E., Torgersen, T., 1986. Chlorine-36 dating of very old groundwater; 1, The Great Artesian Basin, Australia. Water Resour. Res. 22, 1991–2001.

Bethke, C.M., Torgersen, T., Park, J., 2000. The ''age'' of very old groundwater: insights from reactive transport models. J. Geochem. Explor., 1–4.

Biddulph, D.L., Beck, J.W., Burr, G.S., Donahue, D.J., 2006. Two 60-year records of ^{129}I from coral skeletons in the South Pacific Ocean. In: Povinec, P., Sanchez-Cabeza, J.A. (Eds.), Isotopes in Environmental Studies, Proc. Internat. Conf., Monaco, 25–29 October 2004. Radioact. Environ. 8.

Bottomley, D.J., Renaud, R., Kotzer, T., Clark, I., 2002. Iodine-129 constraints on residence times of deep marine brines in the Canadian Shield. Geology 30, 587–590.

Broecker, W.S., Peng, T.-H., 1982. Tracers in the Sea. Eldigio Press, Lamont-Doherty Geol. Obs., Palisades, NY.

Buraglio, N., Aldahan, A., Possnert, G., Vintersved, I., 2001. ^{129}I from the nuclear reprocessing facilities traced in precipitation and runoff in northern Europe. Environ. Sci. Technol. 35, 1579–1586.

Bureau of Land Management, 1999. Coalbed methane development in the northern San Juan Basin of Colorado and New Mexico: A brief history and environmental observations, San Juan Field Office. Available from: <http://oil-gas.state.co.us/Library/sanjuanbasin/blm_sjb.htm>.

Carpenter, L.J., Sturges, W.T., Penkett, S.A., Liss, P.S., Alicke, B., Heberstreit, K., Platt, U., 1999. Short-lived alkyl iodides and bromides at Mace Head, Ireland: Links to biogenic sources and halogen oxide production. J. Geophys. Res. 104, 1679–1690.

Choate, R., Lent, J., Rightmire, C.T., 1984. Upper Cretaceous geology, coal, and the potential for methane recovery from coalbeds in San Juan Basin – Colorado and New Mexico. In: Rightmire, C.T., Eddy, G.E., Kirr, J.N. (Eds.), AAPG Studies in Geology Series: Coalbed methane resources of the United States, vol. 17, Tulsa, OK, pp. 185–222.

Clarkson, G., Reiter, M., Fassett, J.E., 1988. An overview of geothermal studies in the San Juan Basin, New Mexico and Colorado; Geology and coal-bed methane resources of the northern San Juan Basin, Colorado and New Mexico. Denver, CO: Rocky Mountain Assoc. Geologists, pp. 285–292.

Cornett, R.J., Andrews, H.R., Chant, L.A., Davies, W.G., Greiner, B.F., Imahori, Y., Koslowsky, V.T., Kotzer, T., Milton, J.C.D., Milton, G.M., 1997. Is ^{36}Cl from weapons' test fallout still cycling in the atmosphere? Nucl. Inst. Met. Phys. Res. B. 123, 378–381.

Davis, S.N., Cecil, D., Zreda, M., Sharma, P., 1998. Chlorine-36 and the initial value problem. Hydrogeol. J. 6, 104–114.

Davis, S.N., Fabryka-Martin, J., Wolfsberg, L., Moysey, S., Shaver, R., Alexander, E.C., Krothe, N., 2000. Chlorine-36 in ground water containing low chloride concentrations. Ground Water 38, 912–921.

Davis, S.N., Cecil, L.D., Zreda, M., Moysey, S., 2001. Chlorine-36, bromide, and the origin of spring water. Chem. Geol. 179, 3–16.

Decarvalho, H.G., Martins, J.B., Medeiros, E.L., Tavares, O.A.P., 1982. Decay constant for the spontaneous-fission process in ^{238}U. Nucl. Instrum. Meth. Phys. Res. 197, 417–426.

Delmas, R.J., Beer, J., Synal, H.-A., Muscheler, R., Petit, J.-R., Pourchet, M., 2004. Bomb-test ^{36}Cl measurements in Vostok snow (Antarctica) and the use of ^{36}Cl as a dating tool for deep ice cores. Tellus 56B, 492–498.

Edmonds, H.N., Zhou, Z.Q., Raisbeck, G.M., Yiou, F., Kilius, L., Edmond, J.M., 2001. Distribution and behavior of anthropogenic ^{129}I in water masses ventilating in the North Atlantic Ocean. J. Geophys. Res. 106, 6881–6894.

Egeberg, P.K., Dickens, G.R., 1999. Thermodynamic and halogen pore water constraints on gas hydrate distribution at ODP Site 997 (Blake Ridge). Chem. Geol. 153, 53–79.

Elderfield, H., Truesdale, V.W., 1980. On the biophilic nature of iodine in seawater. Earth Planet. Sci. Lett. 50, 105–114.

Elmore, D., Tubbs, L.E., Newman, D., Ma, X.Z., Finkel, R., Nishizumi, K., Beer, J., Oeschger, H., Andree, M., 1982. ^{36}Cl bomb pulse measured in a shallow ice core from Dye 3, Greenland. Nature 300, 735–737.

Fabryka-Martin, J., Bentley, H., Elmore, D., Airey, P.L., 1985. Natural iodine-129 as an environmental tracer. Geochim. Cosmochim. Acta 49, 337–347.

Fabryka-Martin, J.T., Davis, S.N., Elmore, D., Kubik, P.W., 1989. In situ production and migration of ^{129}I in the Stripa granite, Sweden. Geochim. Cosmochim. Acta 53, 1817–1823.

Fabryka-Martin, J., Whittemore, D.O., Davis, S.N., Kubik, P.W., Sharma, P., 1991. Geochemistry of halogens in the Milk River aquifer, Alberta, Canada. Appl. Geochem. 6, 447–464.

Farber, E., Vengosh, A., Gavrieli, I., Marie, A., Bullen, T.D., Mayer, B., Polak, A., Shavit, U., 2007. The geochemistry of groundwater resources in the Jordan Valley: The impact of the Rift Valley brines. Appl. Geochem. 22, 494–514.

Fassett, J.E., 2000. Geology and coal resources of the Upper Cretaceous Fruitland Formation. In: San Juan Basin, New Mexico and Colorado, Geologic Assessment of coal in the Colorado Plateau: Arizona, Colorado, New Mexico, and Utah, Kirschbaym, M.A., Roberts, L.N.R., Biewick, L.R.H. (Eds.), US Geol. Surv. Prof. Pap. 1625-B (Chapter Q).

Fehn, U., Snyder, G., 2000. ^{129}I in the Southern Hemisphere: Global redistribution of an anthropogenic isotope. Nucl. Instrum. Meth. Phys. Res. B 172, 366–371.

Fehn, U., Snyder, G.T., 2005. Residence times and source ages of fluids from the KTB-VB hole, Germany: Interpretation of ^{129}I and ^{36}Cl results. Geofluids 5, 42–51.

Fehn, U., Peters, E.K., Tullai-Fitzpatrick, S., Kubik, P.W., Sharma, P., Teng, R.T.D., Gove, H.E., Elmore, D., 1992. ^{129}I and ^{36}Cl concentrations in waters of eastern Clear Lake area, California: Residence times and source ages of hydrothermal fluids. Geochim. Cosmochim. Acta 56, 2069–2079.

Fehn, U., Snyder, G.T., Egeberg, P.K., 2000. Dating of pore fluids with ^{129}I: Relevance for the origin of marine gas hydrates. Science 289, 2332–2335.

Fehn, U., Snyder, G.T., Matsumoto, R., Muramatsu, Y., Tomaru, H., 2003. Iodine dating of pore waters associated with gas hydrates in the Nankai area, Japan. Geology 31, 521–524.

Fehn, U., Moran, J.E., Snyder, G.T., Muramatsu, Y., 2007. The initial ^{129}I/I ratio and the presence of 'old' iodine in continental margins. Nucl. Inst. Meth. Phys. Res. B, in press.

Fontes, J.-C., Andrews, J.N., 1993. Comment on "Reinterpretation of ^{36}Cl data: physical processes, hydraulic interconnections and age estimate in groundwater systems" by E. Mazor. Appl. Geochem. 8, 663–666.

Gorody, A.W., 2001. Coalbed methane production faces numerous concerns. Oil Gas J. 99, 66–67.

Greenberg, J.P., Guenther, A.B., Turnipseed, A., 2005. Marine organic halide and isoprene emissions near Mace Head, Ireland. Environ. Chem. 2, 291–294.

Heaton, R.K., Lee, H., Robertson, B.C., 1988. Neutron yields in norite based on mineral composition. Sudbury Neutrino Observatory Technical Report SNO-STR-88-101.

Heaton, R., Lee, H., Skensved, P., Robertson, B.C., 1990. Alpha-induced neutron activity in materials. Nucl. Geophys. 4, 499–510.

Hebeda, E.H., Schulz, L., Freundel, M., 1987. Radiogenic, fissiogenic, and nucleogenic noble-gases in zircons. Earth Planet. Sci. Lett. 85, 79–90.

Hedenquist, J.W., Goff, F., Phillips, F.M., Elmore, D., Stewart, M.K., 1990. Groundwater dilution and residence times, and constraints on chloride source, in the Mokai geothermal system, New Zealand, from chemical, stable isotope, tritium, and ^{36}Cl data. J. Geophys. Res. 95, 19365–19375.

Holden, N.E., Zucker, M.S., 1983. Californium-252 and ^{238}U nuclear parameters of safeguards interest. Trans. Am. Nucl. Soc. 45 (Suppl. 1), 23–24.

Hurwitz, S., Mariner, R.H., Fehn, U., Snyder, G.T., 2005. Systematics of halogen elements and their radioisotopes in thermal springs of the Cascade Range, Central Oregon, Western USA. Earth Planet. Sci. Lett 235, 700–714.

Kellett, J.R., Evans, W.R., Allan, G.L., Fifield, L.K., 1993. Reinterpretation of ^{36}Cl data: physical processes, hydraulic interconnections and age estimates in groundwater systems – Discussion. Appl. Geochem. 8, 653–658.

Kennedy, H.A., Elderfield, H., 1987. Iodine diagenesis in pelagic deep-sea sediments. Geochim. Cosmochim. Acta 51, 2489–2504.

Kuuskraa, V.A., Boyer, C.M., 1993. Economic and parametric analysis of coalbed methane. In: Law, B.E., Rice, D.D. (Eds.), AAPG Studies in Geology: Hydrocarbons from Coal, vol. 38, Tulsa, OK, pp. 373–394 (Chapter 17).

Lehmann, B.E., Purtschert, R., 1997. Radioisotope dynamics – the origin and fate of nuclides in groundwater. Appl. Geochem. 12, 727–738.

Lehmann, B.E., Love, A., Purtschert, R., Collon, P., Loosli, H.H., Kutschera, W., Beyerle, U., Aeschbach-Hertig, W., Kipfer, R., Frape, S.K., Herczeg, A., Moran, J., Tolstikhin, I.N., Gröning, M., 2003. A comparison of groundwater dating with ^{81}Kr, ^{36}Cl, and ^{4}He in four wells of the Great Artesian Basin, Australia. Earth Planet. Sci. Lett. 211, 237–250.

Levine, J.R., 1993. Coalification: The evolution of coal as a source rock and reservoir rock for oil and gas. In: Law, B.E., Rice, D.D. (Eds.), Hydrocarbons from Coal, AAPG Stud. Geol. Series 38, pp. 39–77.

Lippmann, J., Stute, M., Torgersen, T., Moser, D.P., Hall, J.A., Lin, L., Borcsik, M., Bellamy, R.E.S., Onstott, T.C., 2003. Dating ultra-deep mine waters with noble gases and ^{36}Cl, Witwatersrand Basin, South Africa. Geochim. Cosmochim. Acta 67, 4597–4619.

Lisitzin, A.P., 1996. Oceanic sedimentation: lithology and geochemistry. In: Translation of Protsessy okeanskoi sedimentatsii, Nauka, Moscow. Kennett, J.P., Biscayne, P., Leinen, M., Sigurdsson, H.,Kennet, D. (Eds.), Woolhiser, C. (Translator), AGU English edition, Washington DC.

Littke, R., Leythaeuser, D., 1993. Migration of oil and gas in coals. In: Law, B.E., Rice, D.D. (Eds.), Hydrocarbons from Coal, AAPG Stud. Geol. Series 38, pp. 219–236.

Lyons, W.B., Welch, K.A., Snyder, G., Olesik, J., Graham, E.Y., Marion, G.M., Poreda, R.J., 2005. Halogen geochemistry of the McMurdo dry valleys lakes, Antarctica: Clues to the origin of solutes and lake evolution. Geochim. Cosmochim. Acta 69, 305–323.

Martin, J.B., Gieskes, J.M., Torres, M., Kastner, M., 1993. Bromine and iodine in Peru margin sediments and pore fluids: Implications for fluid origins. Geochim. Cosmochim. Acta 57, 4377–4389.

Mazor, E., 1992. Reinterpretation of ^{36}Cl data: Physical processes, hydraulic interconnections and age estimates in groundwater systems. Appl. Geochem. 7, 35–360.

Mazor, E., 1993a. Some basic principles of ^{36}Cl hydrology: A reply to the discussion by Kellett, Evans, Allan, and Fifield. Appl. Geochem. 8, 659–662.

Mazor, E., 1993b. Chlorine-36 data and basic concepts of hydrology-Comment on F.M. Phillips' comment, with special reference to the Great Artesian Basin. Appl. Geochem. 8, 649–651.

Mazor, E., Nativ, R., 1992. Hydraulic calculation of groundwater flow velocity and age: Examination of basic premises. J. Hydrol. 138, 211–222.

Mazor, E., Nativ, R., 1994. Stagnant groundwater stored in isolated aquifers: Implications related to hydraulic calculation and isotopic dating – Reply. J. Hydrol. 154, 409–418.

McCord, J., Reiter, M., Phillips, F., 1992. Heat-flow data suggest large ground-water fluxes through Fruitland coals of the northern San Juan basin, Colorado–New Mexico. Geology 20, 419–422.

Meek, R.H., Levine, J.R., 2006. Delineation of Four "Type Producing Areas" (TPAs) in the Fruitland Coal Bed Gas Field of New Mexico and Colorado, Using Production History Data, Search and Discovery Article #20031. Available from: <http://www.searchanddiscovery.net/documents/2006/06025meek/index.htm>.

Moran, J.E., Fehn, U., Hanor, J.S., 1995. Determination of source ages and migration patterns of brines from the US Gulf Coast basin using ^{129}I. Geochim. Cosmochim. Acta 59, 5055–5069.

Moran, J.E., Fehn, U., Teng, R.T.D., 1998. ^{129}I/I ratios in Recent marine sediments: Evidence for a fossil organic source component. Chem. Geol. 152, 193–203.

Moran, J.E., Oktay, S., Santschi, P.H., Schink, D.R., 1999. Atmospheric dispersal of ^{129}Iodine from nuclear fuel reprocessing facilities. Environ. Sci. Technol. 33, 2536–2542.

Moran, J.E., Oktay, S.D., Santschi, P.H., 2002. Sources of iodine and iodine-129 in rivers. Water Resour. Res. 38. doi:10.1029/2001WR00062.

Mughabghab, S.F., Divadeenam, M., Holden, N.E., 1981. Neutron Cross-sections. In: Neutron Resonance Parameters and Thermal Cross-sections, Part A: $Z = 1$–60, Volume 1. Academic Press, New York.

Muramatsu, Y., Fehn, U., Yoshida, S., 2001. Recycling of iodine in fore-arc areas: Evidence from the iodine brines in Chiba, Japan. Earth Planet. Sci. Lett. 192, 583–593.

National Coal Resources Data System, 2006. US Geological Survey Energy Program. Available from: <http://energy.er.usgs.gov/products/databases/CoalQual/index.htm>.

Nolte, E., Krauthan, P., Korschinek, G., Maloszewski, P., Fritz, P., Wolf, M., 1991. Measurements and interpretations of ^{36}Cl in groundwater, Milk River aquifer, Alberta, Canada. Appl. Geochem. 6, 435–445.

Palmer, I.D., Lambert, S.W., Spitler, J.L., 1993. Coalbed methane well completions and stimulations. In: Law, B.E., Rice, D.D. (Eds.), AAPG Studies in Geology: Hydrocarbons from Coal, vol. 38, Tulsa, OK, pp. 303–339 (Chapter 14).

Park, J., Bethke, C.M., Torgersen, T., Johnson, T.M., 2002. Transport modeling applied to the interpretation of groundwater ^{36}Cl age. Water Resour. Res. 38, 1043. doi:10.1029/2001/WR00039, 1-15.

Parrington, J.R., Knox, H.D., Breneman, S.L., Baum, E.M., Feiner, F., 1996. Nuclides and isotopes: Chart of the Nuclides. 15th ed. Lockheed Martin Distribution Services, Cincinatti, OH.

Phillips, F.M., 1993. Comment on "Reinterpretation of ^{36}Cl data: Physical processes, hydraulic interconnections and age estimates in groundwater systems" by E. Mazor. Appl. Geochem. 8, 643–647.

Phillips, F.M., Bentley, H., Davis, S.N., Elmore, D., 1986. Chlorine-36 dating of very old groundwater 2: Milk River Aquifer, Alberta, Canada. Water Resour. Res. 22, 2003–2016.

Phillips, F.M., Zreda, M.G., Smith, S.S., Elmore, D., Kubik, P.W., Sharma, P., 1990. Cosmogenic chlorine-36 chronology for glacial deposits at Bloody Canyon, eastern Sierra Nevada. Science 248, 1529–1532.

Poreda, R.J., Hunt, A.G., Welch, K., Lyons, W.B., 2004. Chemical and isotopic evolution of Lake Bonney, Taylor Valley: Timing of Late Holocene climate change in Antarctica. Aquat. Geochem. 10, 353–371.

Rao, U., Fehn, U., Teng, R.T.D., Goff, F., 1996. Sources of chloride in hydrothermal fluids from the Valles caldera, New Mexico: A ^{36}Cl study. J. Volcanol. Geotherm. Res. 72, 59–70.

Rao, U., Hollocher, K., Sherman, J., Eisele, I., Frunzi, M.N., Swatkoski, S.J., Hammons, A.L., 2005. The use of ^{36}Cl and chloride/bromide ratios in discerning salinity sources and fluid mixing patterns: A case study at Saratoga Springs. Chem. Geol. 222, 94–111.

Rice, D.D., 1993. Composition and origins of coalbed gas. In: Law, B.E., Rice, D.D. (Eds.) AAPG Studies in Geology: Hydrocarbons from Coal, vol. 38, Tulsa, OK, pp. 159–184 (Chapter 7).

Riese, W.C., Pelzmann, W.L., Snyder, G.T., 2005. New insights on the hydrocarbon system of the Fruitland Formation coal beds, northern San Juan Basin, Colorado and New Mexico, USA. In: Warwick, P.D. (Ed.), Geol. Soc. Am. Spec. Pap. 387: Coal Systems Analysis, Golden, CO, pp. 73–111.

Scheffel, C., Blinov, A., Massonet, S., Sachsenhauser, H., Stan-Sion, C., Beer, J., Synal, H.A., Kubik, P.W., Kaba, M., Nolte, E., 1999. ^{36}Cl in modern atmospheric precipitation. Geophys. Res. Lett. 26, 1401–1404.

Schnabel, C., Olive, V., Atarashi-Andoh, M., Dougans, A., Ellam, R.M., Freeman, S., Maden, C., Stocker, M., Synal, H.-A., Wacker, L., Xu, S., 2007. ^{129}I/^{127}I ratios in Scottish coastal surface sea water: Geographical and temporal responses to changing emissions. Appl. Geochem. 22, 619–627.

Schraufnagel, R.A., 1993. Coalbed methane production. In: Law, B.E., Rice, D.D. (Eds.) AAPG Studies in Geology: Hydrocarbons from Coal, vol. 38, Tulsa, OK, 341-359 (Chapter 15).

Schwehr, K.A., Santschi, P.H., Moran, J.E., Elmore, D., 2005. Near-conservative behavior of ^{129}I in the Orange County aquifer system, California. Appl. Geochem. 20, 1461–1472.

Scott, A.R., Kaiser, W.R., Ayers Jr., W.B., 1994. Thermogenic and secondary biogenic gases, San Juan Basin Colorado and New Mexico—Implications for coalbed gas producibility. AAPG Bull. 78, 1186–1209.

Sharma, P., Bourgeois, M., Elmore, D., Granger, D., Lipschutz, M.E., Ma, X., Miller, T., Mueller, K., Rickey, G., Simms, P., Vogt, S., 2000. PRIME lab AMS performance, upgrades, and research applications. Nucl. Instrum. Meth. Phys. Res. B. 172, 112–123.

Snyder, G.T., Fehn, U., 2002. The origin of iodine in volcanic fluids: ^{129}I results from the Central American Volcanic Arc. Geochim. Cosmochim. Acta 67, 3827–3838.

Snyder, G., Fehn, U., 2004. Global distribution of ^{129}I in rivers and lakes: Implications for iodine cycling in surface reservoirs. Nucl. Instrum. Meth. B 223–224, 579–586.

Snyder, G.T., Riese, W.C., Franks, S., Fehn, U., Pelzmann, W.L., Gorody, A.W., Moran, J.E., 2003. Origin and history of waters associated with coal-bed methane: ^{129}I, ^{36}Cl and stable isotope results from the Fruitland Formation, CO and NM. Geochim. Cosmochim. Acta 67, 4529–4544.

Sorek, P., 2003. Evaluation of Helium-4 in a Coalbed Methane System, and Implications for Regional Hydrogeology, Fruitland Formation, Colorado and New Mexico. M.S. Thesis, Colorado State Univ., Fort Collins, CO.

Starinsky, A., Katz, A., 2003. The formation of natural cryogenic brines. Geochim. Cosmochim. Acta 67, 1475–1484.

Synal, H.-A., Beer, J., Bonani, G., Suter, M., Wölfli, W., 1990. Atmospheric transport of bomb-produced ^{36}Cl. Nucl. Inst. Meth. Phys. Res. B. 52, 483–488.

Tomaru, H., Fehn, U., Lu, Z., Matsumoto, R., 2007. Halogen systematics in the Mallik 5L-38 gas hydrate production research well, Northwest Territories, Canada: Implications for the origin of gas hydrates under terrestrial permafrost conditions. Appl. Geochem. 22, 656–675.

Torgersen, T., 1980. Controls on pore-fluid concentration of ^{4}He and ^{222}Rn and the calculation of $^{4}He/^{222}Rn$ ages. J. Geochem. Explor. 13, 57–75.

Torgersen, T., 1994. Hydraulic calculation of groundwater flow velocity and age: examination of the basic premises – Comment. J. Hydrol. 154, 403–408.

Torgersen, T., Kennedy, B.M., van Soest, M.C., 2004. Diffusive separation of noble gases and noble gas abundance patterns in sedimentary rocks. Earth Planet. Sci. Lett. 226, 477–489.

Young, G.B.C., McElhiney, J.E., Paul, G.W., 1991. An analysis of Fruitland coalbed methane production, Cedar Hill Field, Northern San Juan Basin. Soc. Petrol. Eng. Pub. SPE22913, 263–276.

Zhou, Z., Ballentine, C.J., 2006. ^{4}He dating of groundwater associated with hydrocarbon reservoirs. Chem. Geol. 226, 309–327.

Zhou, Z., Ballentine, C.J., Kipfer, R., Schoell, M., Thibodeaux, S., 2005. Noble gas tracing of groundwater/coalbed methane interaction in the San Juan Basin, USA. Geochim. Cosmochim. Acta 69, 5413–5428.

Ziegler, J.F., 1977. Helium Stopping Powers and Ranges in All Elemental Matter. In: The Stopping and Ranges of Ions in Matter, Vol. 4. Pergamon Press, New York.

Zreda, M., Noller, J.S., 1998. Ages of prehistoric earthquakes revealed by cosmogenic chlorine-36 in a bedrock fault scarp at Hebgen Lake. Science 282, 1097–1099.

Zreda, M.G., Phillips, F.M., Kubik, P.W., Sharma, P., Elmore, D., 1993. Cosmogenic ^{36}Cl dating of a young basaltic eruption complex, Lathrop Wells, Nevada. Geology 21, 57–60.